

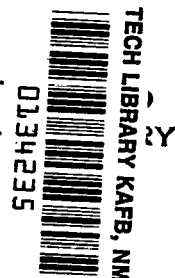
NASA TECHNICAL NOTE



NASA TN D-8502 *c.1*

NASA TN D-8502

LOAN COPY: RE
AFWL TECHNICAL
KIRTLAND AFB,



GSFC SHORT PULSE RADAR, JONSWAP-75

*D. M. Le Vine, W. T. Walton, J. Eckerman,
R. L. Kutz, M. Dombrowski, and J. E. Kalshoven, Jr.*

*Goddard Space Flight Center
Greenbelt, Md. 20771*





0134235

1. Report No. TND-8502		2. Government Accession No.		3. Recipient's Catalog No.	
4. Title and Subtitle GSFC Short Pulse Radar, JONSWAP-75		7. Author(s) D. M. Le Vine et al.		5. Report Date June 1977	
9. Performing Organization Name and Address Goddard Space Flight Center Greenbelt, Maryland 20771		12. Sponsoring Agency Name and Address National Aeronautics and Space Administration Washington, D. C. 20546		6. Performing Organization Code 950	
15. Supplementary Notes		16. Abstract In September 1975, the Goddard Space Flight Center operated a short pulse radar during ocean-wave measuring experiments off the coast of West Germany in the North Sea. The experiment was part of JONSWAP-75. This document describes the radar system and operations during the experiment and presents examples of data.		8. Performing Organization Report No. G-7702-F11	
17. Key Words (Selected by Author(s)) Radar, Nanosecond pulse radar, Ocean Wave experiment, JONSWAP-75		18. Distribution Statement Unclassified—Unlimited Cat. 35		10. Work Unit No. 161-03-02	
19. Security Classif. (of this report) Unclassified		20. Security Classif. (of this page) Unclassified		11. Contract or Grant No.	
				13. Type of Report and Period Covered Technical Note	
				14. Sponsoring Agency Code	
				21. No. of Pages 42	
				22. Price* \$4.00	

All measurement values are expressed in the International System of Units (SI) in accordance with NASA Policy Directive 2220.4, paragraph 4.

CONTENTS

	<i>Page</i>
ABSTRACT	i
INTRODUCTION	1
RADAR SYSTEM	6
EXPERIMENT SITE AND OPERATIONS	20
EXAMPLES OF DATA	26
CONCLUSIONS	31
REFERENCES	32
APPENDIX A—FLIGHT LOG	37

GSFC SHORT PULSE RADAR, JONSWAP-75

**D. M. Le Vine, W. T. Walton, J. Eckerman,
R. L. Kutz, M. Dombrowski, and J. E. Kalshoven, Jr.**
*Goddard Space Flight Center
Greenbelt, Maryland*

INTRODUCTION

Interest in ocean-measuring spacecraft has risen sharply in recent years with recognition of their potential for synoptic measurement of transient and large-scale ocean phenomena. The scientific reward from such measurements can be expected to accrue to many disciplines, and includes better analytic models of ocean dynamics, such as currents, tides, sea state, and coastal processes, as well as better models for oceanic topology and the geoid and improved understanding of air/sea interactions. Economic benefits and benefits expected to accrue to all people of the world include increased safety and efficiency of ocean-going traffic, improved forecasting of sea state with an incumbent improvement in safety to coastal regions, and improvements in the environment through increased understanding and through pollution monitoring.

A specific example of how satellite data may affect present practice is wave forecasting. Current practice is based on ship reports of winds at sea. The forecasting program is initialized with a wave spectrum obtained from a hindcast procedure using this wind field. Using the actual observed wave field obtainable from satellite monitoring for model initialization would result in a more accurate forecast and a reduction in computation.

Among the many sensors that show promise for remote sensing of ocean surface parameters are microwave devices. These are especially appropriate for monitoring surface structure because they penetrate cloud cover and interact strongly with waves.

Among the systems being considered for wave measurements is a short pulse real-aperture radar being developed at the Goddard Space Flight Center (GSFC). This radar transmits a short pulse of microwave radiation from an antenna that points near nadir and that has a narrow "pencil" beam for obtaining resolution in azimuth. The short pulse radar has several important features, including: the potential for simple onboard processing that results in low data rates; the concomitant potential for a near real-time measurement system; and the potential for use as a basic general-purpose radar that is capable of performing scatterometry (to obtain wind speed), operating in an altimetry mode to obtain sea state, and measuring wave structure, as well as possibly being applicable to problems of ice and snow monitoring.

The use of a short pulse radar to measure wave structure is not a particularly new idea. It dates to at least the late 1950's. For example, in 1958, Meyers (Reference 1), using an X-band radar mounted on a tower on the Atlantic coast, demonstrated a temporal correlation between wave-staff measurements and the modulation of power scattered back to the receiver. This work was done at incidence angles near grazing. More recently, Zamarayev and Kalmykov (Reference 2) presented data and corroborating analysis that supports a similar observation at larger incidence angles.

Tomiyasu (Reference 3) suggested the use of the short pulse radar concept for satellite application. He proposed that the spectrum of large-scale ocean waves could be related to modulation of the range-time display (A-scan) of the radar when operated from a satellite. He was not specific about the scattering mechanism and suggested a spectrum analyzer as the signal processor.

The basic concept behind the short pulse radar is illustrated in figure 1. The sensor radiates a short pulse with duration, τ , (about 10 ns) and spatial width, $c\tau$ (c = speed of light), from an antenna whose beamwidth is θ_b and which points at an angle, θ_n , from the normal to the mean surface. When the pulse reaches the surface, it intersects a length, $c\tau/(\sin \theta_n)$, on the mean surface, and, as the pulse propagates forward, its intersection with the surface moves across the beam's "footprint" (i.e., the illuminated portion of the surface). If $c\tau/(\sin \theta_n)$ is smaller than the wavelength of the dominant wave mode on the surface, then the pulse intersects the surface at different local angles as it moves across the footprint. Consequently, the scattered power would be expected to change as a function of time in some manner corresponding to the waves on the surface as shown in figure 1.

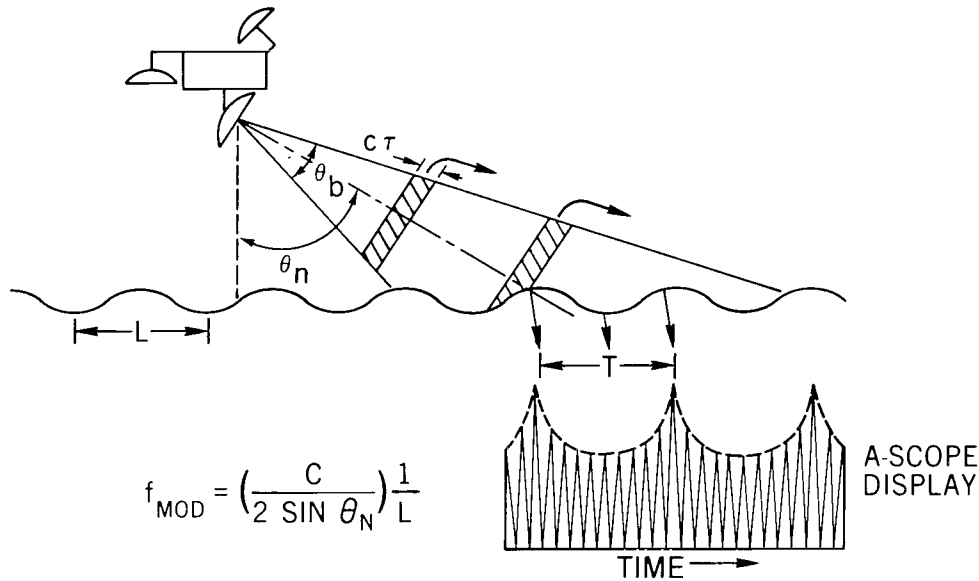


Figure 1. Ocean sensing concept using a short pulse radar.

Remote sensing of waves from an airplane or satellite using this radar technique differs from ground-based sensing, primarily in geometry. The larger range to the surface with remote systems results in a wider illumination of the surface (footprint), although increasing antenna dimensions can partially overcome this effect. Clearly, when the projection of the radar pulse on the ocean surface illuminates only a small section of the ocean waves, then modulation of the radar signal would closely follow the ocean-wave structure. However, when the transverse extent of the footprint (i.e., perpendicular to figure 1) is much larger than the ocean-wave crest length, the radar signal is expected to be reduced—i.e., the modulation depth decreased. Since ocean-crest length is a function of wavelength, the effect of too wide illumination is to reduce the signal for the shorter waves. The ocean-crest length is on the order of three times ocean wavelength, L . For a platform at altitude, h , looking out at a nadir angle, θ_n , with radar wavelength, λ , the antenna diameter, D , that under-illuminates waves transverse to the plane of incidence is:

$$D = \frac{h \lambda}{3 L \cos(\theta_n)}$$

Figure 2 shows this antenna diameter plotted as a function of altitude for a 30° nadir angle. From aircraft altitudes (10 km), antennas less than 1 m in diameter can resolve 50-m waves at either 1 or 2 cm wavelengths. A 14-m antenna at $\lambda = 1$ cm could resolve 100-m waves from shuttle altitudes. However, at proposed oceanographic spacecraft altitudes (polar orbit at 700 km), the shortest waves that this 14-m antenna would properly illuminate have a 200-m wavelength when the radar wavelength is 1 cm. The performance of the radar for waves shorter than 200 m may be satisfactory, although this point requires test and demonstration and is one of the elements of the present research program.

Several studies have been performed to examine the performance of this radar technique. Brooks and Dooley (Reference 4) pointed out some constraints on sensor performance: (1) the pulse length projected on the ocean surfaces should be smaller than the shortest ocean wavelength of interest; (2) wave-front curvature in the radar footprint on the ocean surface limits the smallest usable nadir angle; and (3) the shortest resolvable wave is a function of the modulation index of the received signal, the signal bandwidth, and the pulse bandwidth.

Jackson (Reference 5) performed a general detection-system analysis, treating the wave scattering as modulated noise. Le Vine* modeled the response of the ocean to a short radar pulse. In the latter report, the ocean was considered to be a stochastic corrugated surface, the Kirchhoff approximation was employed, and it was shown that wave information was obtainable from the envelope of the spectrum of the received power.

In addition to these studies, GSFC conducted some early tests of the short pulse radar concept with the help of the Naval Research Laboratory (NRL) (References 6 and 7). In

*D. M. Le Vine, "Spectrum of Power Scattered by a Short Pulse from a Stochastic Surface," NASA/GSFC X-952-74-299, April 1974.

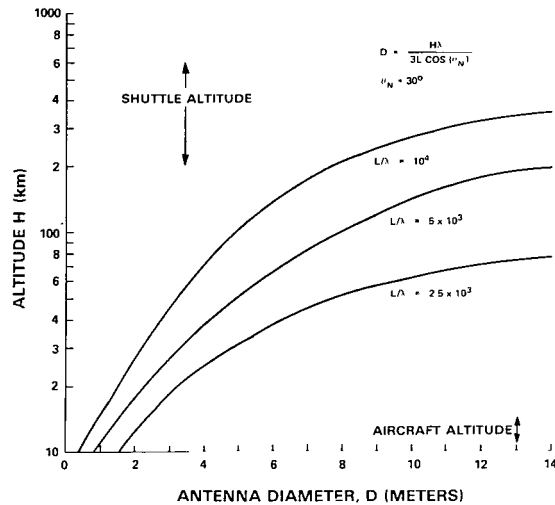


Figure 2. Critical antenna diameter for sensing ocean waves as a function of altitude.

September 1973, during JONSWAP-73, an NRL X-band altimeter was flown for several flights in a short pulse mode, and, in January 1974, a modified system was flown in the short pulse mode off the Atlantic Coast of the United States.

The NRL X-band altimeter operates at 9.75 GHz with a pulse-repetition frequency of 90 kHz and a variable pulse width (References 8 and 9). Pulses approximately 10 ns long were used in the short pulse experiment, and the antenna for these experiments had a beamwidth of about 6° . The NRL radar "recreates" the signal scattered from a single transmitted pulse by sampling from a sequence of transmitted pulses with samples taken at progressively later times. That is, transmitted pulse 1 is sampled at t_1 , and the next transmitted pulse is sampled at $t_2 > t_1$, and so forth, until signals at all times of interest have been recorded. It requires $1/90$ second to complete the sampling procedure.

It is important to observe that the digital samples are not derived from the return from a single radar pulse but rather that this system obtains its samples from the return (scattered signal) of 1000 pulses sampled sequentially. Because the sea surface is changing with time and is not flat, no unique correspondence exists in such a system between a scan as recorded on tape and the signal returned from any single pulse. In order for such a relationship to exist, with the signal-sampling technique used with the NRL radar, a number of assumptions must be made: First, it must be assumed that the signal received from any individual pulse doesn't change in the $1/90$ second required to produce one complete scan. Obviously, there is a difference between the two measurements if the surface has changed during this time interval. Second, it is necessary to assume that the surface heights are small; if not, the scatter received as a function of (increasing) time does not always come from positions on the surface of increasing distance from the receiver. This problem may arise on a surface with waves that are large compared to the wavelength (of the radar's signal) when the antenna beam is pointing off-nadir.

The first data taken with the NRL radar altimeter were during JONSWAP-73 over the North Sea in September 1973. In these flights, the radar was mounted in its nadir-pointing (i.e., altimeter) position in the belly of the National Aeronautics and Space Administration (NASA) Wallops Flight Center C-54. To obtain data with the beam pointing at angles off-nadir, the aircraft was put into a banked turn. Data were obtained in this manner at angles of 10° and 15° with the aircraft at about 3 km. Of course, as a result of the turning, the antenna's beam is continually changing with respect to the wind direction, and there is also some uncertainty in the beam-pointing angle.

Following the JONSWAP-73 flights, the radar's antenna was mounted on a movable platform with a port on the side of the aircraft for pointing the antenna. This permitted straight-line flights at a fixed orientation with respect to the wind and at more precisely defined beam-pointing angles. In addition, the signal-to-noise ratio of the radar was improved for these flights.

Data were taken in this configuration during January 1974 over seas off the mid-Atlantic Coast of the United States. A "star" pattern was flown to obtain data at various orientations with respect to the wind direction. Again, data were taken at about 3 km with a 6° horn and with the beam pointing at about 15 degrees from nadir. References 6, 7, and 10 describe these experiments and the data obtained.

Results obtained during these first aircraft experiments were encouraging; however, as previously mentioned, the NRL radar was an altimeter and was therefore not particularly suited to the short pulse radar goals. The radar capability was limited to very low altitude flights and small nadir angles. Also, the low transmitter power required the use of a sampling receiver. Demonstration of the technique for spacecraft implementation required acquisition of data from higher altitudes with narrow, fan-beam antennas, and high power for single-pulse processing.

Accordingly, GSFC made a commitment to design a radar to meet specific short pulse radar needs. Because funds restricted the options, it was eventually decided to convert an available GEOS-C (Geodetic Earth-Orbiting Satellite) breadboard radar altimeter into a working short pulse radar. Further funding restrictions required an almost entirely in-house effort. The result resembled the original breadboard only in a very nominal way (for example, in their common center frequency, 13.9 GHz). The conversion from a disorganized breadboard to working short pulse radar required hard work and long hours performed under the pressure of a very short time schedule.

The resultant high-power Ku-band radar was tested in August 1975 and was able to meet the deadline for participation in JONSWAP-75 scheduled for September 1975. The time from the GSFC commitment to build a dedicated radar until the system was airborne was less than 1 year.

The JONSWAP experiment for 1975 provided an ideal opportunity to test the short pulse radar concept over well-instrumented oceans. The radar was to be mounted in a C-130 aircraft, shared with the NASA/Langley Research Center (LaRC), and flown at various orientations with respect to wind and waves over a section of ocean instrumented by the JONSWAP team under the direction of the Max-Planck-Institut für Meteorologie, Hamburg, West Germany. The primary surface truth consisted of data from an array of wave riders and wind sensors, plus the laser profilometer and camera aboard the aircraft. In addition, a central platform (called "Pisa") was instrumented with radar, optical, and surface-monitoring instrumentation to perform several NASA/LaRC experiments. Of course, there would be the opportunity to compare results with the NASA/LaRC RadScat and Dual-Frequency Scatterometer with which the C-130 was being shared.

Therefore, the objective of the JONSWAP-75 mission was to operate for the first time a true short pulse radar in its various possible modes and to compare the surface-wave estimates with "surface truth" and the measurements of other surface sensors. Accordingly, data were obtained in the off-nadir mode, using various combinations of antennas and look angles, and at nadir, using a nadir-pointing horn. In each case, data were obtained at several orientations with respect to wind and waves. Raw data were recorded in a manner appropriate for processing in either the "wave spectrometer," "scatterometer," or "altimeter" mode. Good data were obtained under several wind and wave conditions, although desirable very high seas did not occur during the experiment period. Algorithms for reducing these data have been written and data reduction is well underway.

The purpose of this report is to document details of the radar system as it existed during JONSWAP-75 (some improvements have been made since then) and to describe the operations and data obtained during the JONSWAP-75 experiment. At this writing, data processing is still underway, and it is expected that reports of results will be forthcoming. The emphasis here is on documenting the experiment.

This report is divided into three parts: The first section describes the radar, including the electronics, data-handling system, and antennas. The second section describes the JONSWAP-75 experiment, the experiment site, and operations during the experiment period. The final section describes the data obtained during the experiment.

RADAR SYSTEM

Background

On the basis of the experience gained from the early tests using the NRL altimeter (References 6 and 7), GSFC decided to build a short pulse radar operating near X-band that would record the power scattered by a single pulse. The breadboard for the GEOS-C microwave radar altimeter was available, and a decision was made to try to build a radar from these

components. GSFC acquired the breadboard, salvaged the RF components, and built the radar. In addition, a special data-handling system was constructed to permit recording of the entire temporal history of the power scattered by a single transmitted pulse, and to permit real-time display of the received signal.

A block diagram, by functional element, of the complete system is shown in figure 3. The received pulse is digitized and stored by the A/D unit, which is a transient analyzer (Biomation Model 8100). The digital data are then transferred to digital tape and can also be viewed on the cathode ray tube (CRT). The primary function of the computer is to control the transient analyzer and the data flow between the transient analyzer and the digital tape and between either of these elements and the display CRT. Software was also provided to permit processing of the stored data during the experiment.

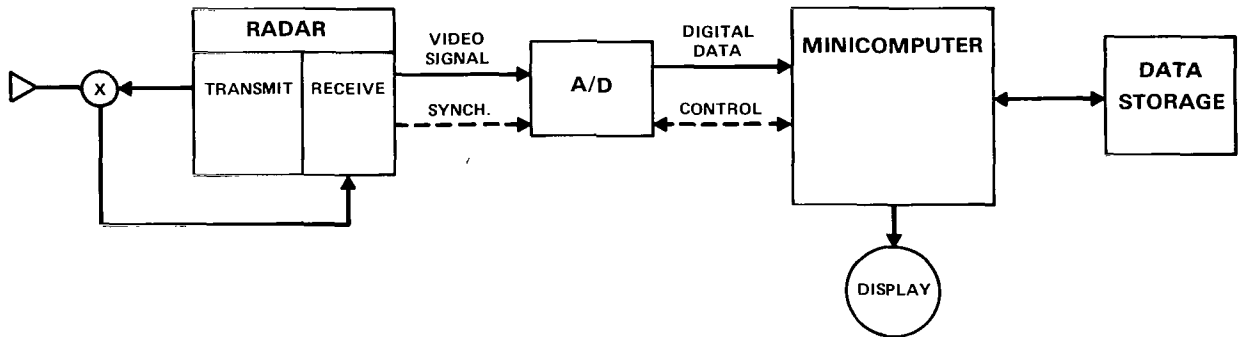


Figure 3. Block diagram of the radar system.

Each of the elements identified in the block diagram will be described in more detail in the following paragraphs.

Radar Electronics

Figure 4 is a block diagram of the radar electronics. The 5-MHz oscillator is used to generate both a 300-MHz signal that drives the chirp generator and the basic 13.6-GHz center frequency of the transmitted pulses. The chirp generator, by means of a diode switch and a surface acoustic wave device, converts the 300-MHz signal into a sequence of 1- μ s wide linearly frequency-modulated pulses (250 to 350 MHz) occurring at a 100-Hz rate. These pulses are mixed with the 13.6 GHz and amplified by two traveling-wave tubes (TWT's) in tandem. The first TWT is operated CW, and the second is grid-pulsed and has a peak power of about 1 kW. The resultant 1-kW chirped pulse at 13.9 GHz is fed to the antenna system, a small amount being tapped off for testing.

On reception, the scattered pulse is amplified, compressed (again using a surface acoustic wave device), and then fed to a square-law detector and video amplifier. The received signal

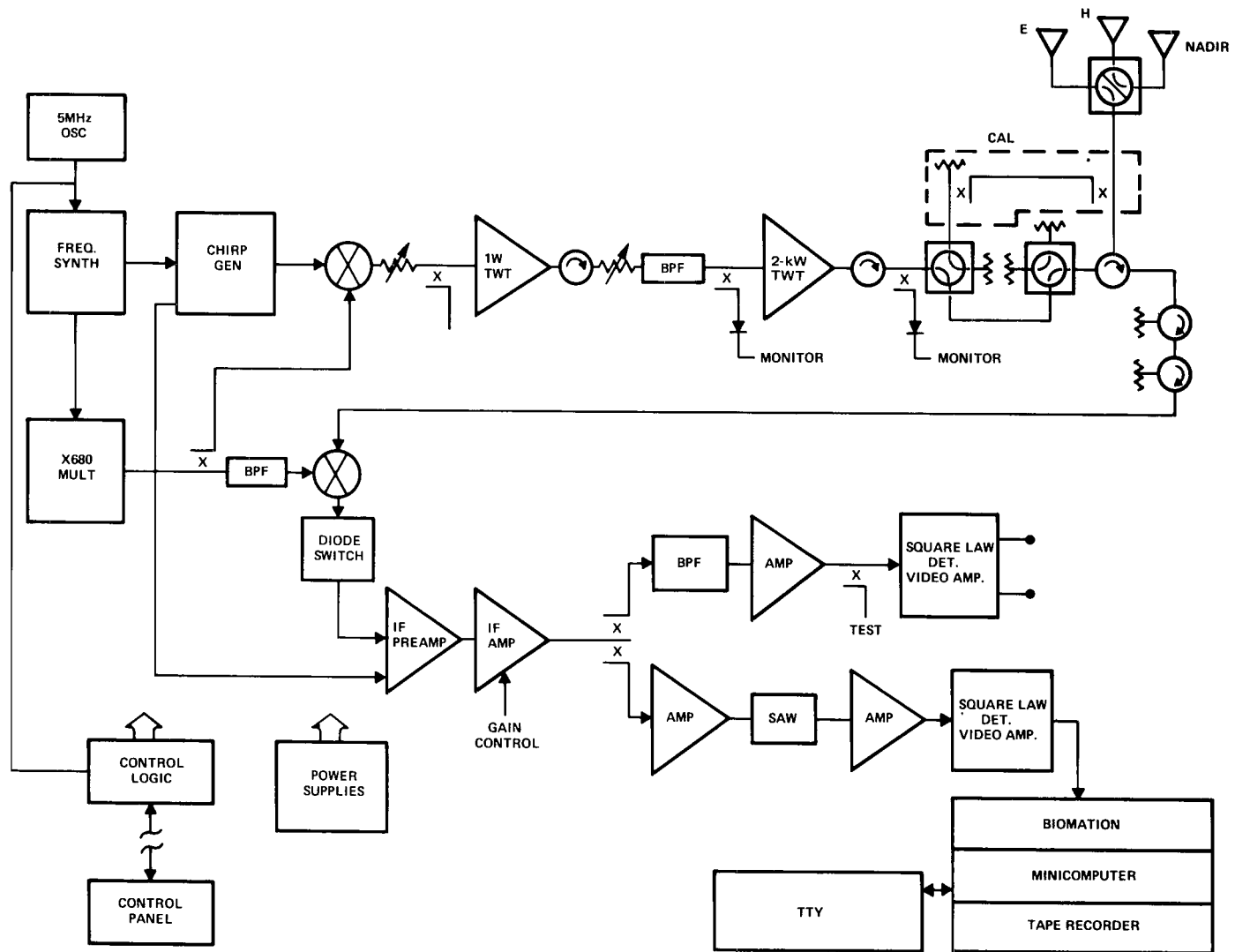


Figure 4. Block diagram of the radar electronics.

is also detected without compression and is available for testing and automatic gain control input, and for recording as data, although it has not been recorded in any of the flights made to date.

The radar electronics were packaged in a Hoffman steel enclosure meeting National Electrical Manufacturers Association standards (figures 5 and 6) with outside dimensions of 76 by 61 by 41 cm. Figure 5 is a view of the box opened and loaded with electronics. Figure 6 identifies the various radar elements and shows their placement inside the box. The most convenient method of packing was to mount the system components to flat plates, with emphasis on accessibility and ease of modification for this experimental unit. The location and orientation of various elements was determined on the basis of minimizing interference and signal paths.

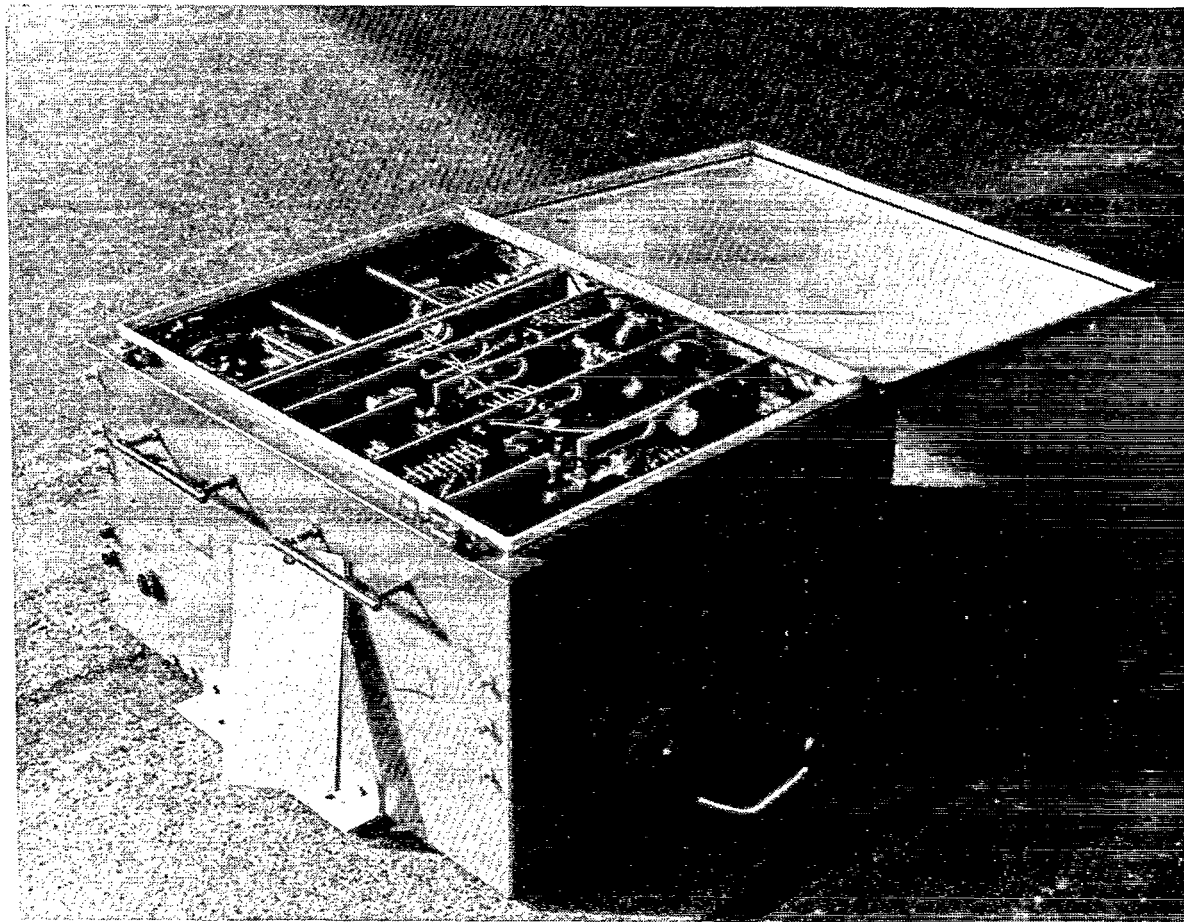


Figure 5. Enclosure for the radar electronics.

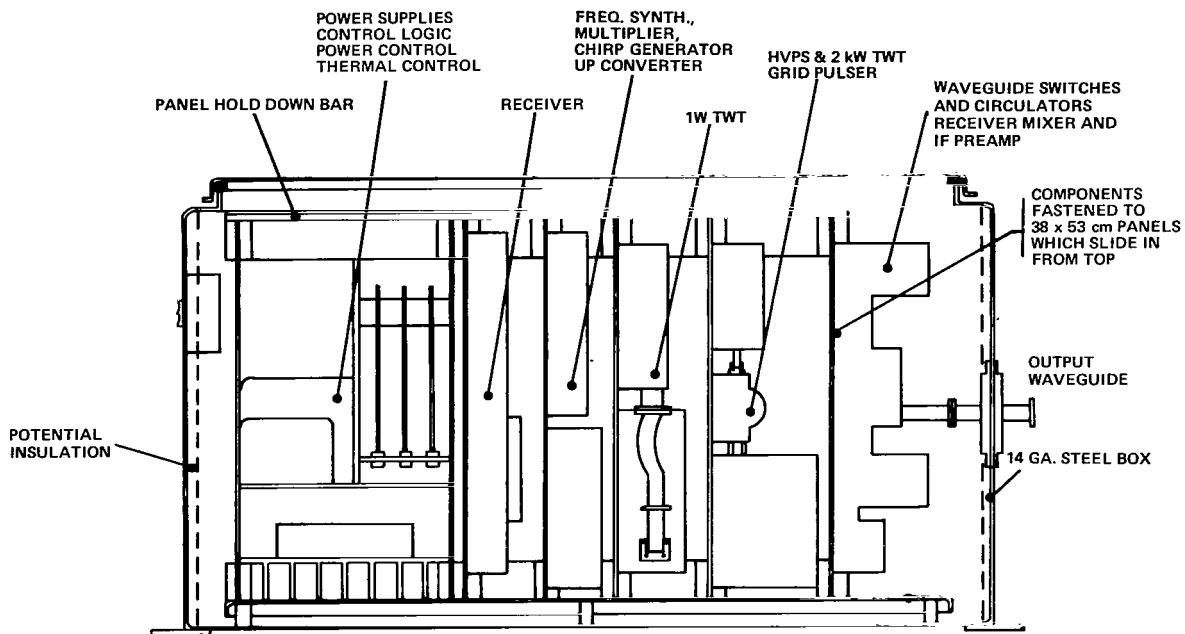


Figure 6. Side-view cross section of radar in enclosure.

The short pulse radar characteristics are:

Composite parameters:

Output tube	TWT
Peak tube power	2.5 kW maximum
Frequency	13.9 GHz
Pulse type	Linear FM coded pulses
Pulse repetition rate	100 pulses per second
Pulse compression type	Linear FM
Uncompressed pulse width	1- μ s minimum
Compressed pulse width	10-ns minimum; 15-ns maximum
Pulse compression ratio	100:1 minimum
Implementation	
Pulse expander	Dispersive delay line at IF of 300 MHz in transmitter chain
Pulse compressor	Dispersive delay line at IF of 300 MHz in receiver chain

Component characteristics:

Front end	
Type	Direct down conversion with image enhanced single ended mixer
Mixer/preamp noise figure	7 dB estimated
Receiver dynamic range	Greater than 70 dB with gain control
Gain control dynamic range	50 dB minimum
IF Section	
IF center frequency	300 MHz
IF filter bandwidths	100-MHz minimum
Detector	
Type	Square-law
Square-law range	20-dB minimum

Antennas

Three antennas were used during the JONSWAP-75 experiment: “E- and H-plane” stick antennas designed for off-nadir use and a nadir-pointing horn. These antennas were used for both transmitting and receiving pulses. The stick antennas were 0.76 m by 10.2 cm and produced a beam of about $2^\circ \times 26^\circ$. These antennas were oriented so that their long physical dimension was parallel to the axis (fuselage) of the airplane, resulting in a beam with small azimuthal extent but large in range. For example, referring to figure 1 and imagining the airplane to be traveling perpendicular to the plane of the figure, then azimuth refers to the dimension perpendicular to the page, and range is the horizontal dimension illustrated in the figure. Thus, θ_b would be 26 degrees for these antennas. The vertically polarized antenna (called H-plane stick in the experiment log) produces electric fields parallel to the plane of figure 1, and the horizontally polarized antenna (called E-plane stick in the experiment log) produces an electric field perpendicular to this plane and therefore parallel to the mean sea surface. (Note that the labels “H-plane” stick and “E-plane” stick as used in the original flight log book are the reverse of the conventional definition.) The stick antennas were mounted so that the pointing angle (angle that the beam center makes with the vertical, θ_n in figure 1) could be varied from flight to flight. The nominal setting used during most of JONSWAP-75 was 18 degrees. In this configuration, there is essentially no return from nadir.

Figures 7 through 12 show the antenna patterns for the stick antennas. Figures 7 and 10 are patterns in the plane perpendicular to long axis of the antenna, and figures 8 and 11 show the azimuthal pattern of the vertically polarized and horizontally polarized antennas, respectively. Figures 9 and 12 are the same azimuthal patterns with an expanded angular scale.

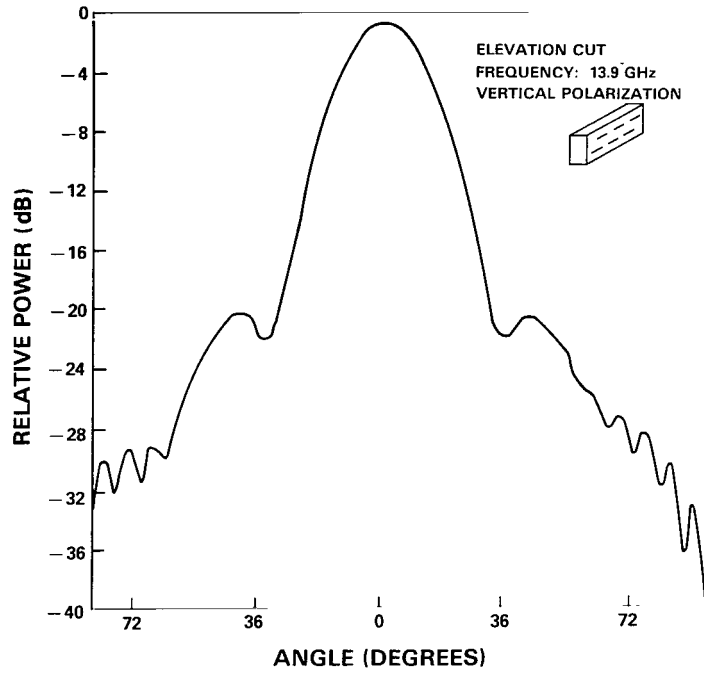


Figure 7. Antenna pattern in elevation, vertical polarization.

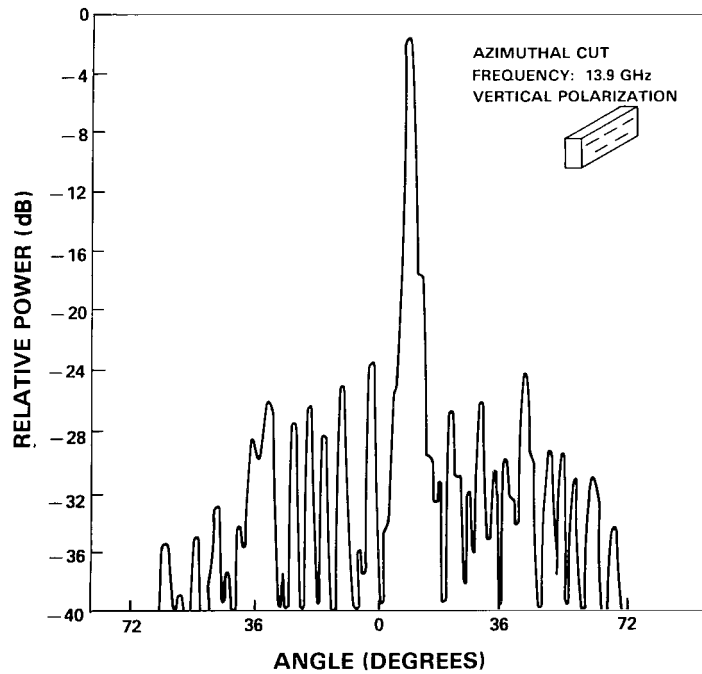


Figure 8. Antenna pattern in azimuth, vertical polarization.

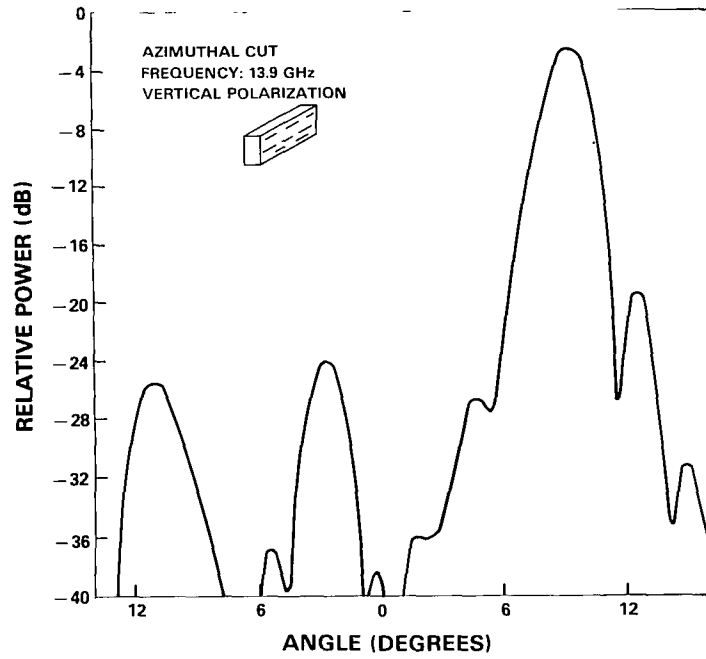


Figure 9. Antenna pattern in azimuth, vertical polarization (expanded scale).

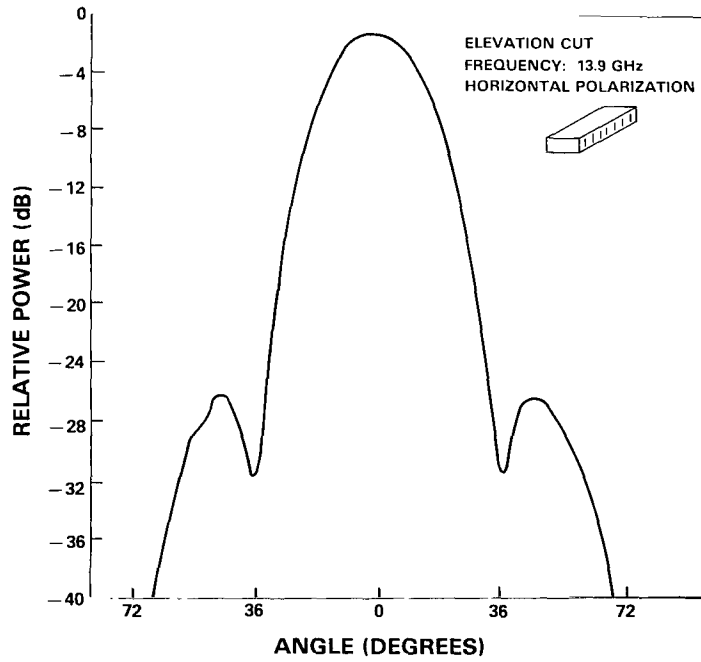


Figure 10. Antenna pattern in elevation, horizontal polarization.

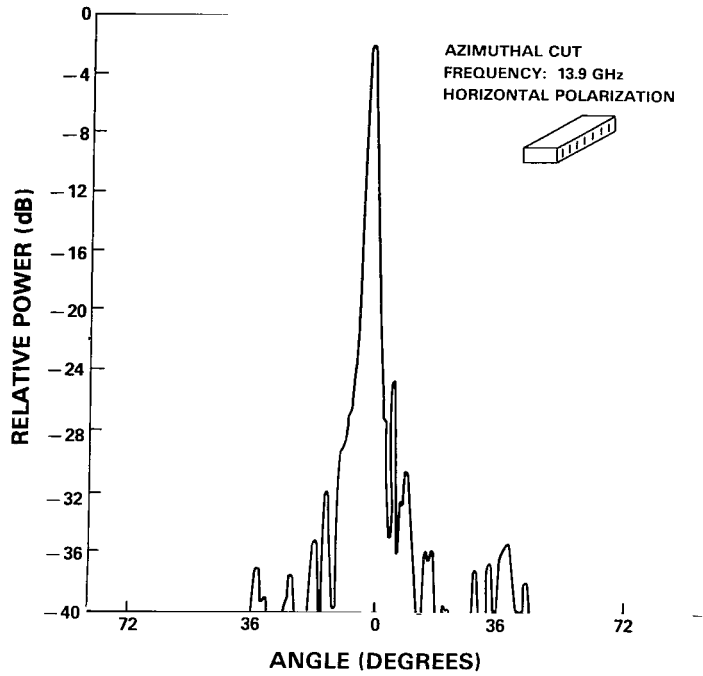


Figure 11. Antenna pattern in azimuth, horizontal polarization.

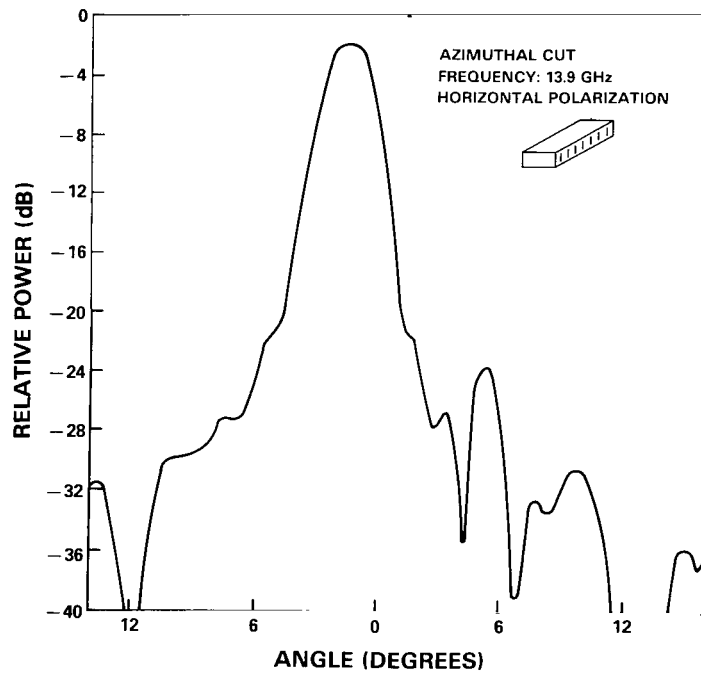


Figure 12. Antenna pattern in azimuth, horizontal polarization (expanded scale).

The nadir horn, a 13.9-GHz standard gain horn, had a half-power beam width of about 20° (10° to each side of the beam center). Figure 13 shows antenna patterns for this horn. The pattern for this horn is reasonably symmetric about the beam axis.

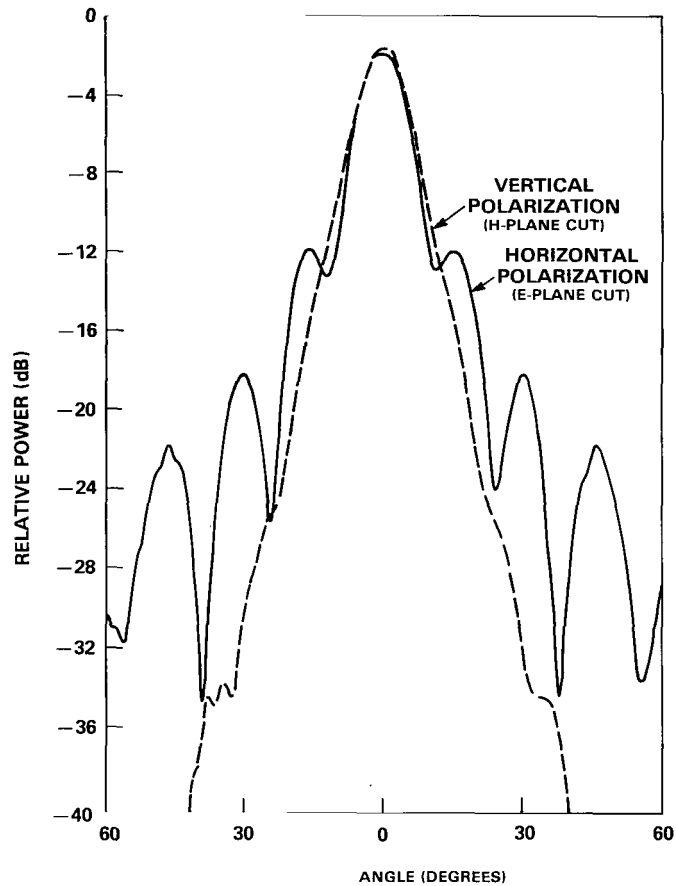


Figure 13. Antenna pattern for the nadir horn.

Figure 14 shows the radar and antenna arrangement on the C-130 A-frame structure.

Analog-to-Digital Conversion

An important consideration in the design of the short pulse radar was the requirement to record the complete history of a single pulse as it scattered from the surface (as opposed to reconstructing this history by sampling from a succession of transmitted pulses). This was accomplished by feeding the video output of the radar directly into a Biomatic transient recorder (Model 8100). This device is capable of sampling the received signal at one sample per 10 ns and storing up to 2000 samples. The data window that this provided was sufficient to capture a complete record of the scattered pulse, with the antennas employed, for altitudes

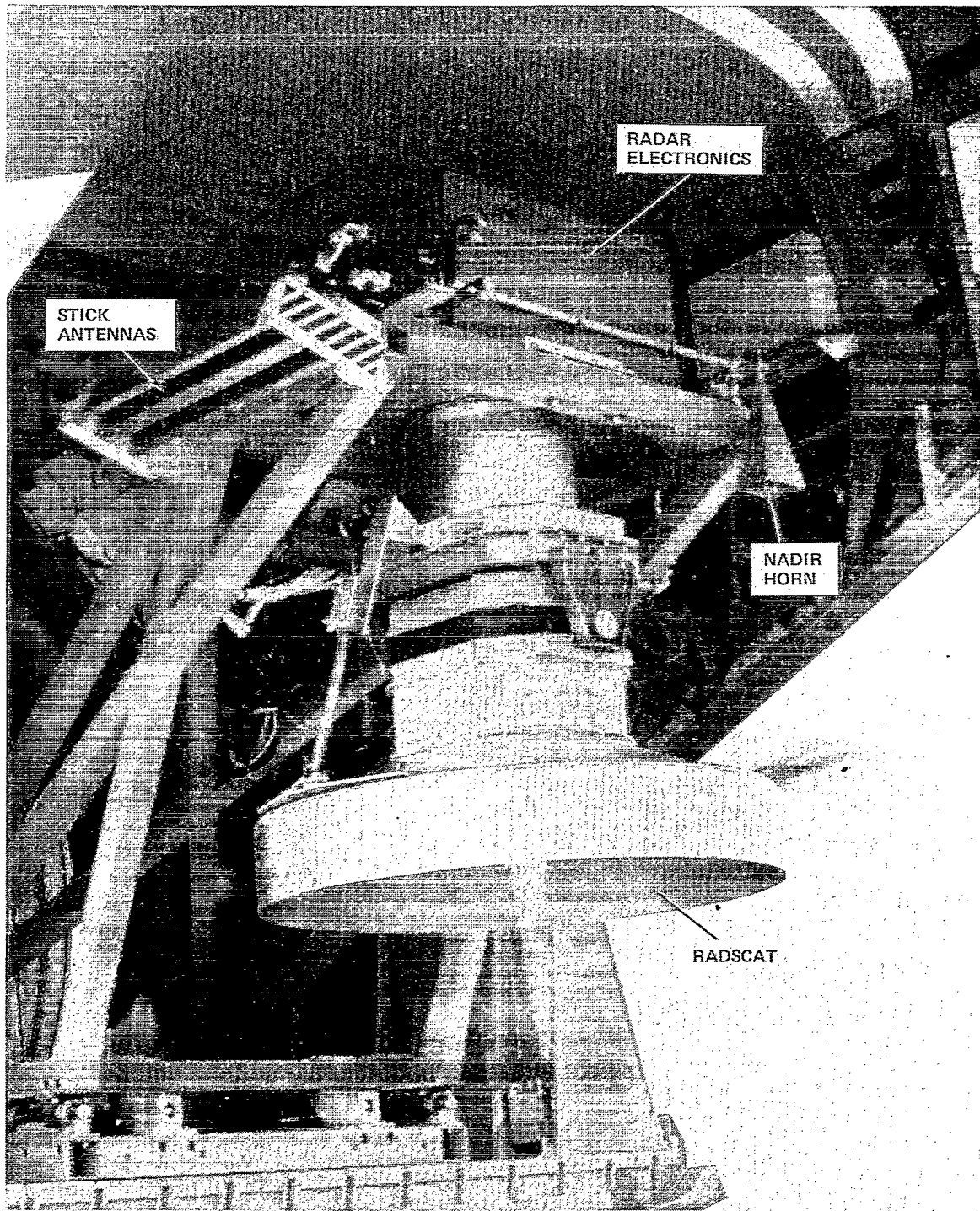


Figure 14. Radar installation on the A-frame in the C-130.

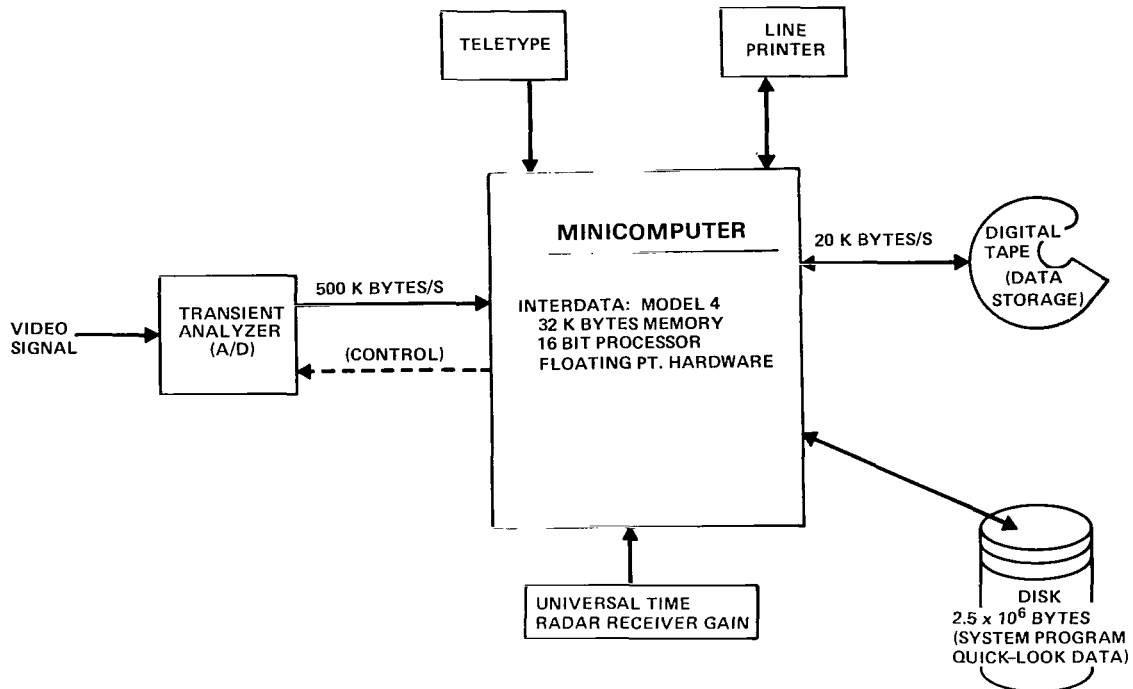


Figure 15. Schematic of the data-handling subsystem.

up to about 12 km. Because none of the altimeter (i.e., ranging) circuitry was retained from the GEOS-C breadboard, the pulse in this window had to be located manually. For this purpose, a real-time display of the signal stored in the transient analyzer was provided on a CRT, and, by adjusting the time delay before triggering the transient recorder, the operator could assure acquisition of the scattered pulse.

The transient analyzer provided digital output of the stored signal at about 200 k bytes/s, which was dumped into computer memory and then stored on magnetic tape.

Data-Handling System

Figure 15 is a block diagram of the data-handling system. The central element in this was an Interdata Model 4 minicomputer that controlled the flow of digital data to and from the storage units. The computer peripherals consisted of a digital tape for eventual storage of the digitized pulses, a disk on which were stored the system software and programs for quick-look analysis and presentation of the data, and a CRT for displaying the received pulses. The system also included a line printer to facilitate programming the computer and to print the results of data analysis (e.g., pulse spectra and averages).

The transient recorder was capable of recording received pulses at the 100-Hz rate at which they were transmitted. However, the available digital tape unit could not operate at the required data rates. Thus, the procedure during operation was to use the computer memory as

a buffer to store the data during transfer to the tape. This permitted two modes of operation: (1) a burst mode in which pulses were recorded at the 100-Hz rate until the memory was filled, or (2) a steady-state mode in which pulses were skipped until the recorded pulse was transferred to tape. Only the steady-state mode was used during the JONSWAP-75 experiment.

The received pulse was also fed to the CRT so that the operator could confirm that a proper pulse had been received. The operator could adjust time delay and gain (quantizing level) in the transient analyzer until a complete pulse of some reasonable peak amplitude appeared in the 20- μ s window. After being set, the adjustments were not changed for a given data run and were recorded as part of the data record. The time delay was especially sensitive to aircraft altitude, as well as attitude.

Because of the relatively slow data rate of the tape recorder, only about 6 pulses could be recorded per second. However, the pulses did not fill the full 20- μ s window. By discarding the empty ends of this window, the rate at which pulses were recorded eventually increased to about 25 pulses per second. (That is, only about 500 of the 2000 samples recorded by the transient analyzer actually transferred to tape for storage.)

Mounting on the Airplane

The C-130 aircraft used for JONSWAP-75 was a cargo carrier outfitted primarily to accommodate the NASA/LaRC dual-frequency scatterometer (DFS). The antenna for the scatterometer was mounted on an A-frame that was rolled out of the cargo door entrance to collect data. The cargo door was opened during flight, and data were taken with the antenna looking either down or at various angles to the side of the plane.

The short pulse radar electronics (the Hoffman NEMA box) and antennas were mounted on the A-frame, and the data-handling system and radar controls were housed in standard equipment racks in the interior of the plane. Figures 14 and 16 show views of the mounting on the A-frame, and figure 17 shows the placement of the radar box on top of the A-frame. The large disk that dominates the center of all three figures and hangs down from the A-frame is the antenna for the DFS. The short pulse radar electronics box is mounted directly above this antenna (figures 14 and 17) and the short pulse radar antennas are mounted to the sides of the box (figure 14). The nadir horn was eventually moved from its position in figure 14 to a position near the end of the stick antennas to help minimize interference with the DFS antenna.

Figure 18 shows the data-handling equipment inside the airplane. The Biomation transient analyzer is at the top of the left panel, and the right panel contains the computer and peripheral systems.

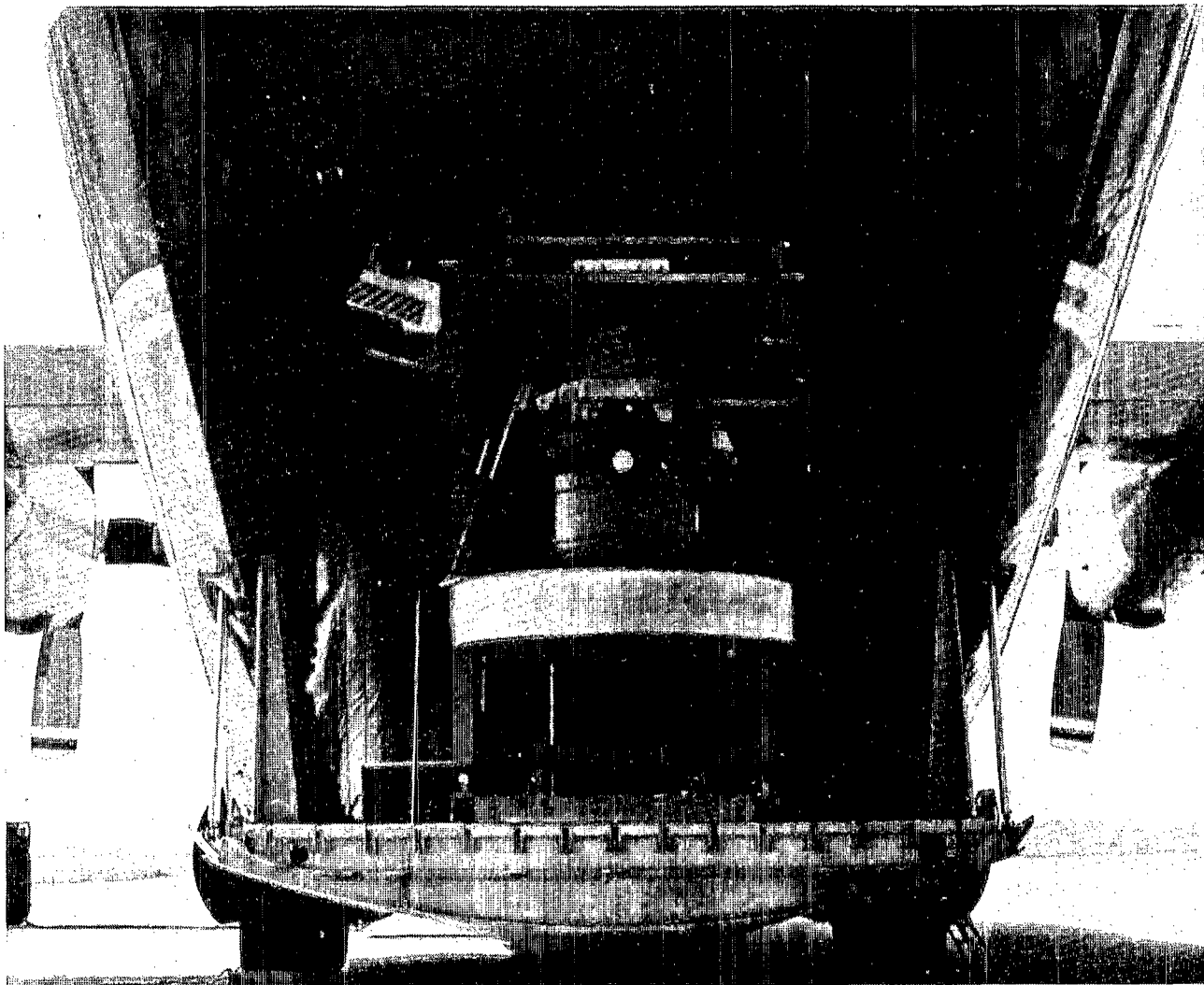


Figure 16. Radar installation in the C-130.

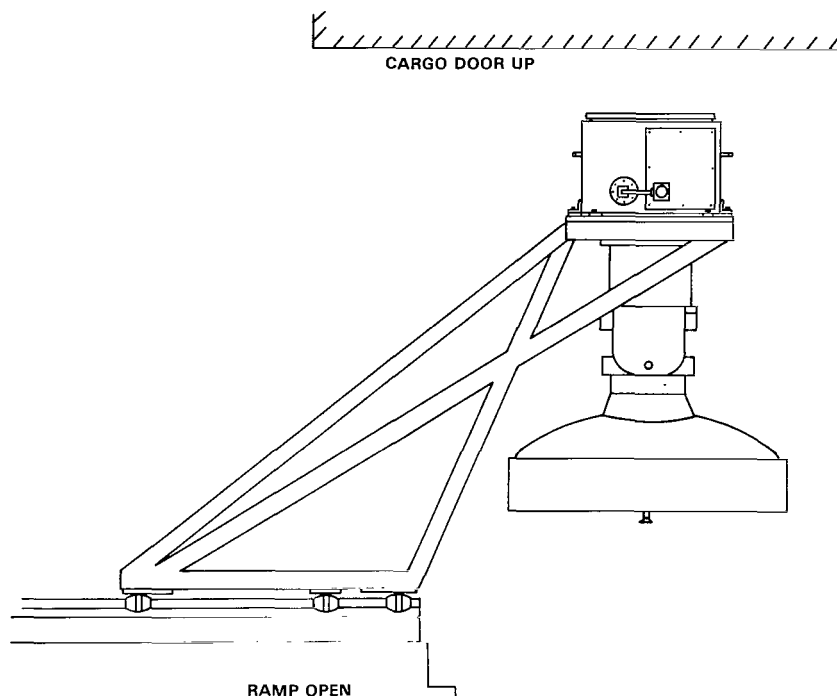


Figure 17. Operational placement of the radar electronics on the A-frame.

EXPERIMENT SITE AND OPERATIONS

Experiment Site

The JONSWAP-75 experiments were performed at an instrumented site off the island of Sylt, which is in the North Sea just south of the boundary between West Germany and Denmark. (See figures 19 and 20). The experiment site consisted of a section of ocean extending west and slightly north from the coast of Sylt. An array of wave-measuring devices (primarily wave riders and wave buoys) were available to measure wave spectra at several sites and a central tower (station 8, called Pisa) was also instrumented with additional devices to measure surface parameters at close range. The surface instrumentation was located at eight stations arranged along a line running northwest (287 degrees) from Sylt (figure 20). The closest station (station 2) on this line was 2 km from shore and consisted of a wave rider. The next station (station 5), consisting of a wave-gage array, was located along the northwest line at 6.5 km from shore. Two wave-rider stations were next (stations 5N and 5S) along a line perpendicular to the northwest line, 10 km on either side of a point 9.5 km from shore. The tower called Pisa (station 8) was located 27 km from shore. Located at the tower were wave riders that provided non-directional wave spectra, a wave staff, a capillary wave probe, an anemometer for windspeed and direction, a wave follower buoy, thermometers for air and sea temperature, and, under the direction of NASA/LARC, a camera for Stilwell photography and a 9.3-GHz radar. To the north (station 8N) and to the south

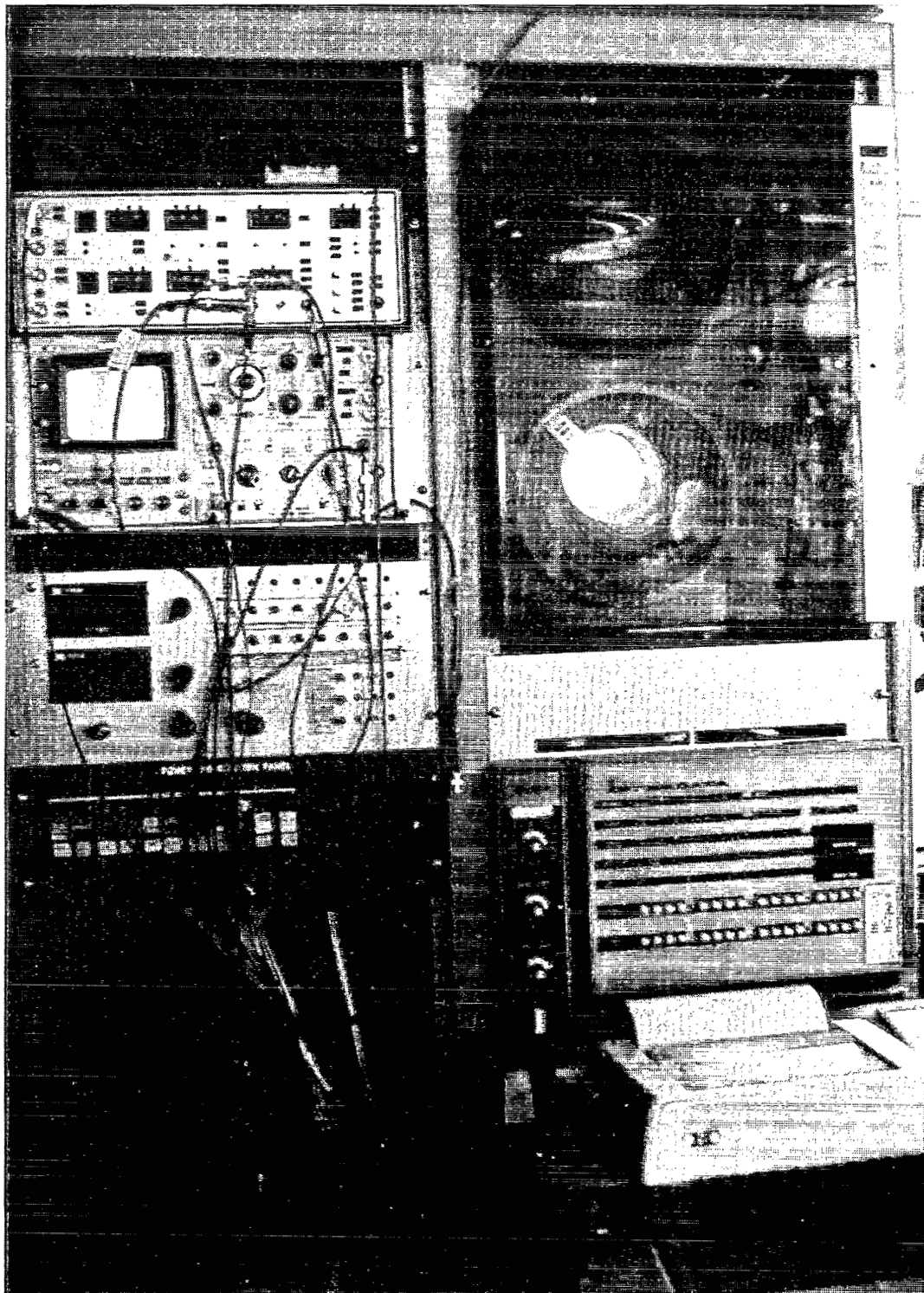


Figure 18. Data-handling system and radar controls.

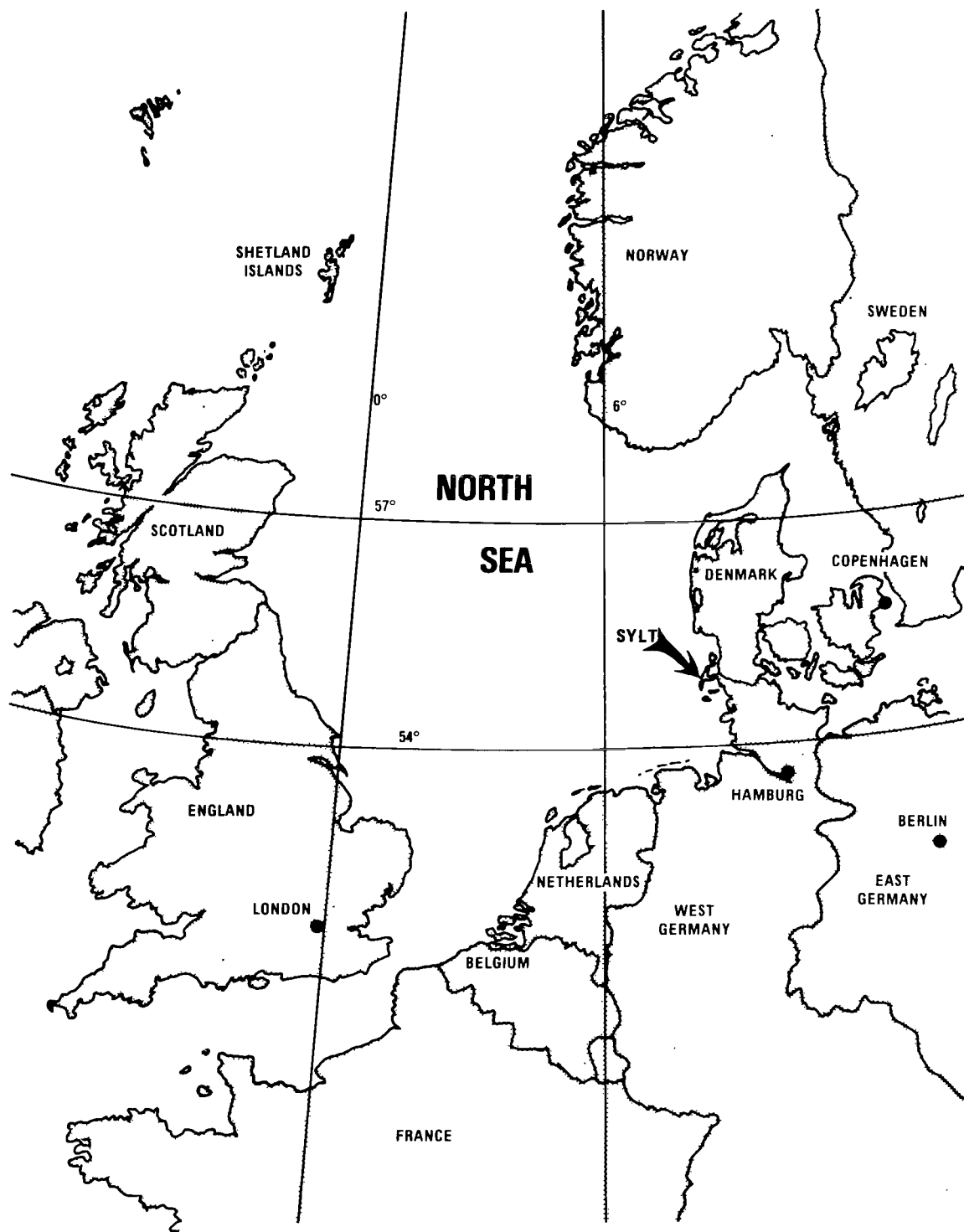


Figure 19. Map indicating the location of Sylt (the experiment site) in the North Sea.

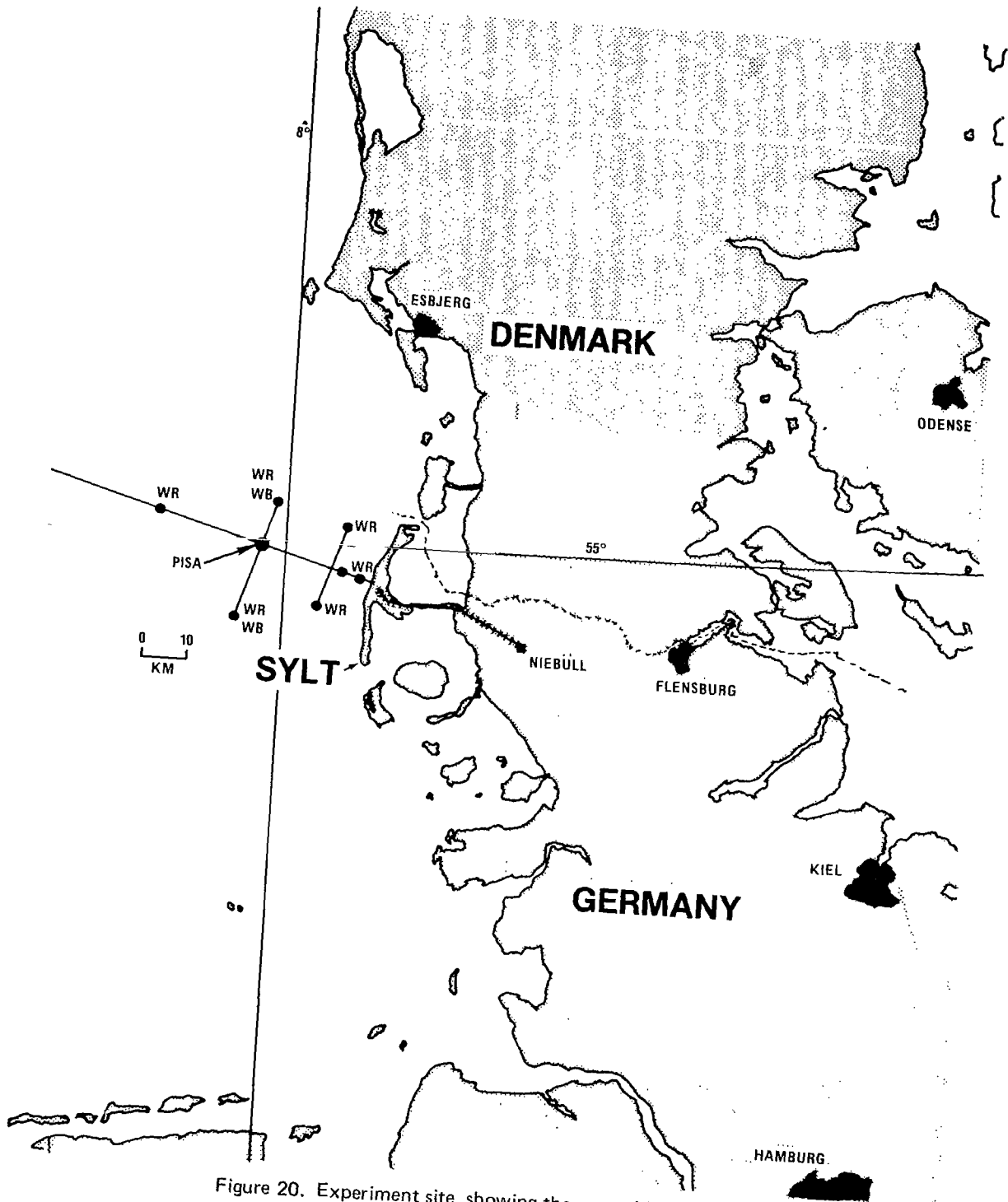


Figure 20. Experiment site, showing the wave rider stations in a northwest grid off the coast of Sylt.

(station 8S) of Pisa were wave riders and wave/wind buoys. Station 8N was 10 km from Pisa and station 8S was 20 km from Pisa, both along a line perpendicular to the main north-west line. The final station (station 10) consisted of a wave rider 52 km from shore. In addition to these fixed stations, an assortment of ships and aircraft assisted in making surface measurements at various periods during the experiment. The "surface truth" is being coordinated by Professor Klaus Hasselmann through the University of Hamburg and will be documented in the final JONSWAP-75 reports (scheduled for the summer of 1977).

In addition to the short pulse radar and the NASA/LaRC dual-frequency scatterometer, the airplane carried a laser profilometer and a nadir-pointing camera for photographing the surface (figure 21).

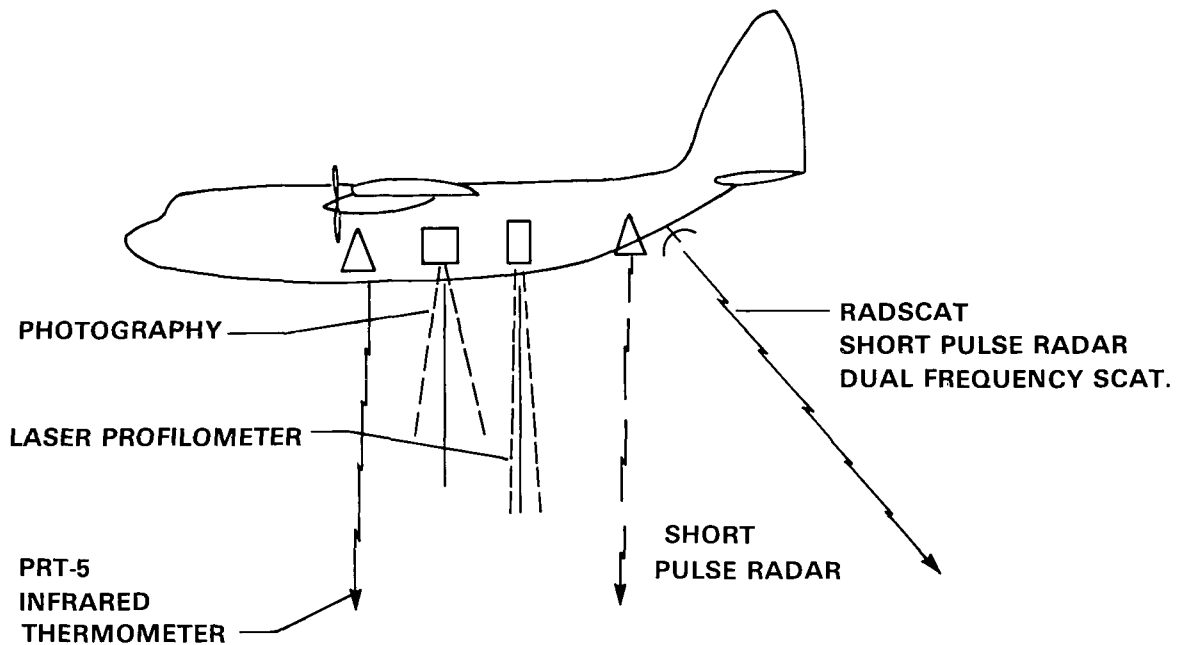


Figure 21. JONSWAP-75 sensors on C-130 aircraft.

Flights

A typical flight began with a low-altitude pass at about 152 m (500 feet) during which the laser profilometer took data over the section of sea of interest. This was followed by a high-altitude (about 1800 to 3000 m) pass during which either the dual-frequency scatterometer or the short pulse radar acquired data.

A particular experiment day was broken up into "flight lines" which consisted of circles and straight-line segments oriented in a predetermined manner with respect to the waves. The straight-line segments included paths perpendicular and parallel to the waves and at

45 degrees to the waves. (See figure 22.) The flight crew established orientation by visual inspection of the surface. Because the seas were often very mixed, visual determination of wave direction was difficult.

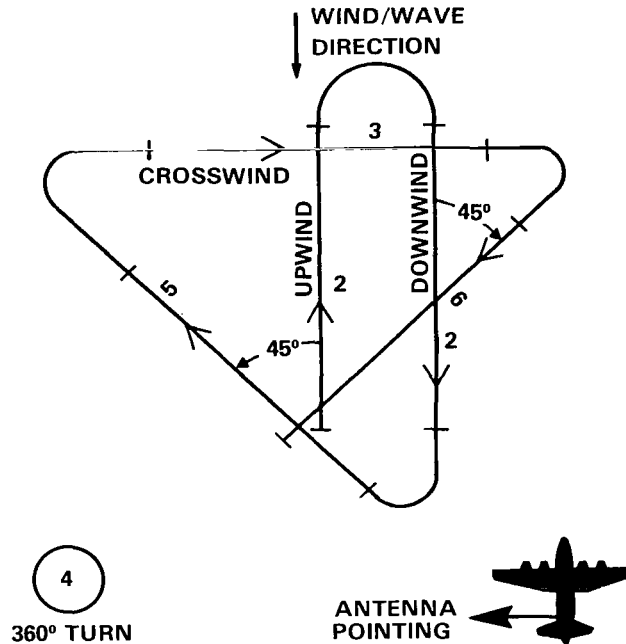


Figure 22. JONSWAP-75 flight-line number and direction.

Because the short pulse radar and the dual-frequency scatterometer could not operate simultaneously without interference, flight lines had to be shared. In the earliest flights, this was done by assigning part of a given line to each party, but it later proved more feasible to assign an entire line to one experiment. Although flight lines were rotated, one sensor was designated “primary” for each day. The camera was operated during all flight lines whenever cloudcover permitted.

A total of 13 flights were originally scheduled (Monday through Thursday for 3.5 weeks) and, for the most part, had to be flown during the morning because of conflicting military operations in the area. Of the 13 flights scheduled, nine were actually flown. Of these, one was an extra flight added to the original schedule. Four flights were cancelled. The decision to fly or not was made jointly by the pilot and principal investigators on the basis of sea state and weather conditions. Of the cancelled flights, one was cancelled because of bad weather, one because of low sea states, and two because of various equipment problems.

The first stage in a given flight consisted of a low-altitude pass (152 meters) over the experiment area during which the laser profilometer and cameras acquired data. (The short pulse radar could not acquire pulses at altitudes below about 437 meters.) The aircraft then proceeded to an altitude of 1830 to 3050 meters and entered one of the flight "lines" for data gathering with either the dual-frequency scatterometer or the short pulse radar. The camera continued to collect data whenever feasible. During these runs, aircraft parameters from the inertial navigation system were being recorded.

An attempt was made to obtain short pulse radar data representative of the various antenna configurations and flight lines. Figure 23 is a chronological list of the data obtained, showing for each day the flight lines for which data were obtained and the antennas employed. Figure 24 is a composite of the entire experiment showing, as a function of altitude, antenna, and flight line, which data were obtained. Finally, table 1 illustrates the sea conditions (estimated) under which data were obtained with each antenna. The flight log (Appendix A) gives a more complete record of the data.

EXAMPLES OF DATA

The raw data product obtained by the short pulse radar during JONSWAP-75 was the power scattered by a single pulse as it moved across the surface. Variables that effect these data include: the antenna used, its beam-pointing angle, the orientation of the flight path with respect to the waves, and the sea state.

The power returned to the nadir horn is a relatively narrow pulse that lasts approximately 40 nanoseconds. Figure 25 shows examples of a succession of pulses received during a run perpendicular to the waves. The pulses shown were separated by 0.12 seconds and were recorded on September 8, 1975, at an altitude of about 2 km. The estimated wave height for this period was about 1 meter. Figure 26 shows an average pulse obtained for this particular flight line by averaging about 2000 pulses. The shape of the initial portion (rise) of the average pulse can be related to significant wave height when the wave amplitudes are normally distributed, and processing is now underway to compare the estimate of significant wave height obtained from such data with the ground truth. One problem of immediate concern in this respect is the wave resolution available with the shortest detectable rise time. With 10 nanoseconds between samples, the minimum spatial resolution is on the order of 3 meters, which would represent relatively high seas.

The data obtained with the stick antennas (that is, data obtained off-nadir) are somewhat different from data observed with the nadir horn. Figure 27 shows examples of a succession of three pulses obtained during a flight oriented at 45 degrees with respect to the waves. Again, the time between pulses is about 0.12 second. These data were recorded on September 9, 1975, at an altitude of about 2 km using the horizontally polarized stick antenna with the beam center at 18 degrees from nadir. Note the rapid rise of power when the pulse first encountered the surface, followed by a period of strong return during which specular scatter determined by the large-scale surface structure was dominant, and followed by a gradual decrease in return. As the pulse moves away from the radar, increasingly large (local)

DATE	TIME	ANT.			LINE		REMARKS
		H	E	N	L	⊙	
24 AUG	PM	●			●		FIRST TRIAL ATLANTIC NEAR HAMPTON, VA.
29 AUG	AM	●			●		FIRST NORTH SEA DATA SHARED RUNS; TEMP. SHUTDOWN
2 SEP	AM	●	●	●	●	●	TEMP. SHUTDOWN BEFORE LINES COMPLETE
4 SEP	AM	●			●		EARLY TEMP. SHUTDOWN. LOCATED TEMP. SEN. CONNECTION.
8 SEP	PM	●		●	●	●	HORN USED AS FAN ON BANK
9 SEP	AM	●	●		●	●	
9 SEP	PM	●			●		
10 SEP	NOON	●		●	●	●	
15 SEP	AM		●		●	●	HEATERS INSTALLED PRIOR TO FLIGHT
16 SEP	AM	●	●	●	●	●	
17 SEP	PM	●	●	●	●	●	FAN BEAMS RAISED TO HIGHER ANGLE, BANKED DOWN. AIRCRAFT INTERCEPTION.

Figure 23. JONSWAP-75 flight summary.

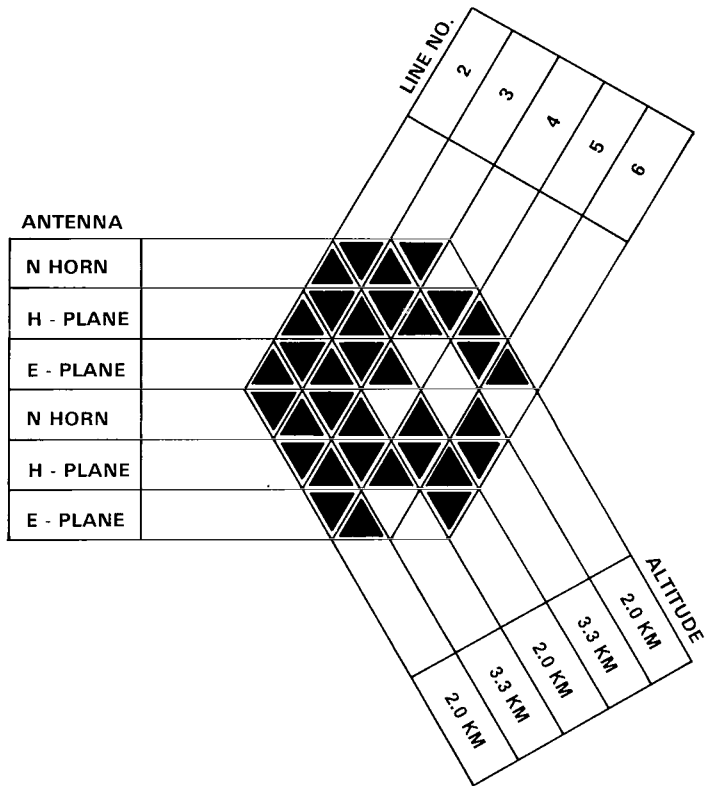


Figure 24. Summary of data collected during JONSWAP-75.

Table 1
Summary of Estimated Surface Conditions

Wave Conditions (meters)	Number of Files*			Total
	E	H	N	
0.3	5			5
0.3 to 1.0	2	2	1	5
1.0 to 1.2	5	4	8	17
1.2 to 1.5	10	8		18
1.5 to 2.1	3			3
2.4 to 3.1	7	1	3	13
	1**	1**		
				61

*A file represents 500 to 1000 pulses.

**E and H stick antennas at 31°, otherwise, antennas at 18°.

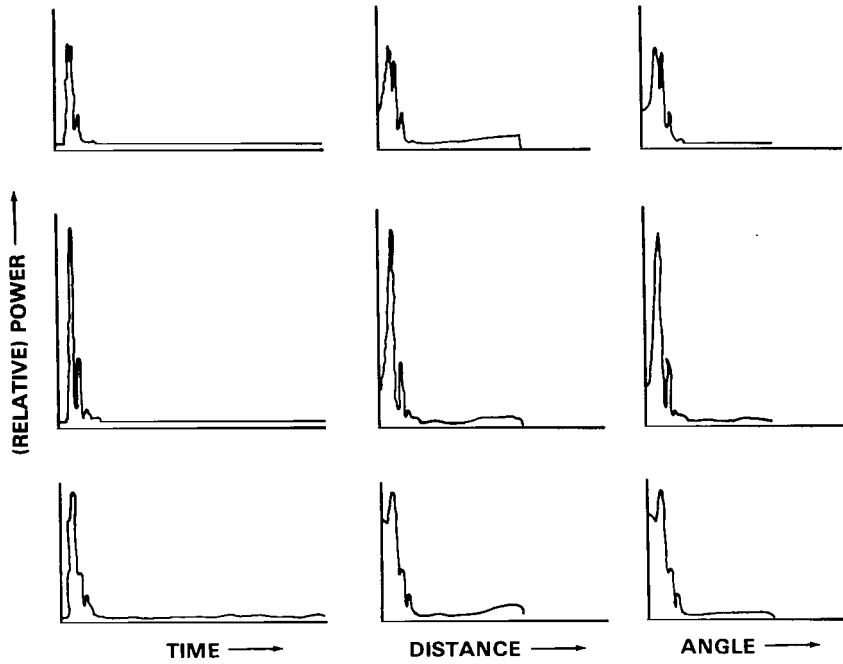


Figure 25. Sample data collected with the nadir horn on September 8, 1975. The aircraft was flying at approximately 6000 feet and perpendicular to the waves.

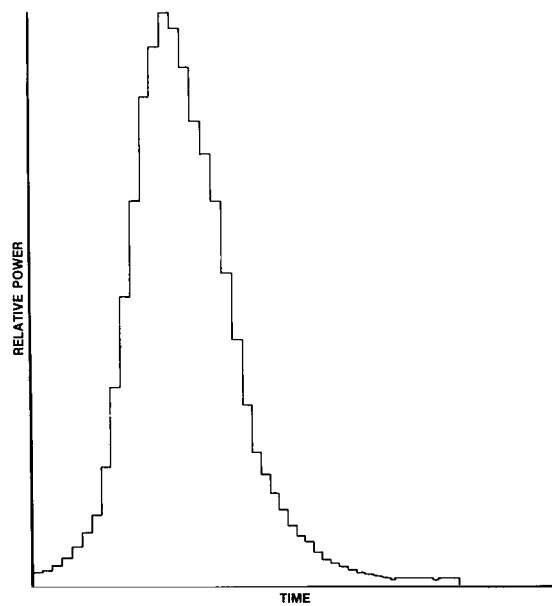


Figure 26. Average pulse of 3000 successive pulses obtained with the nadir horn on September 8, 1975.

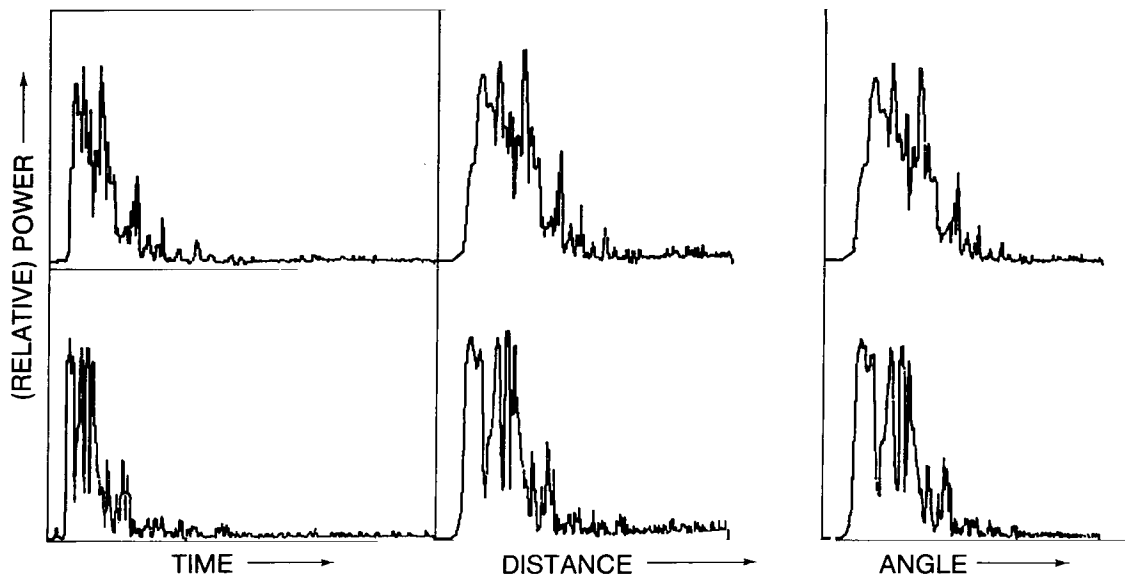


Figure 27. Examples of pulses received September 9, 1975, using the horizontally polarized antenna. The aircraft was flying at about 2 km and at 45° with respect to the waves. The beam center pointed 18 degrees off-nadir. Data are presented for power as a function of time, distance along the surface, and angle in degrees from nadir.

angles of incidence are necessary for backscatter. The probability of such slopes decreases rapidly and, as a result, the dominant scatter mechanism gradually changes from specular scatter (physical optics) to Bragg scatter. According to theory and experiment (References 11 and 12), this transition should occur at incidence angles of around 20° . The data are in reasonable agreement with this conclusion. Examples of average pulses are shown in figure 28. The average pulse has been plotted as a function of time, distance along the surface, and angle of the intersection from nadir. (Because the antenna-surface geometry and the speed of propagation of the signal are known, the time of arrival can be related to a specific distance along the mean surface, and the angle that the line from this point to the radar makes with the vertical can be determined.)

A great deal of work must still be done before comparison of the data with surface truth will be complete. Theories are being developed to determine how best to extract surface parameters from the data,* and these will be compared with spectra and wind fields provided by the JONSWAP-75 oceanographers.

*D. M. Le Vine, "Spectrum of Power Scattered by a Short Pulse from a Stochastic Surface," NASA/GSFC X-952-74-299, April 1974; and R. O. Harger and D. M. Le Vine, "Microwave Radar Sea Sensing of Intermediate Incidence Angles," NASA/GSFC X-952-75-228, September 1975 (accepted for publication in IEEE Transactions on Aerospace Electronics Systems).

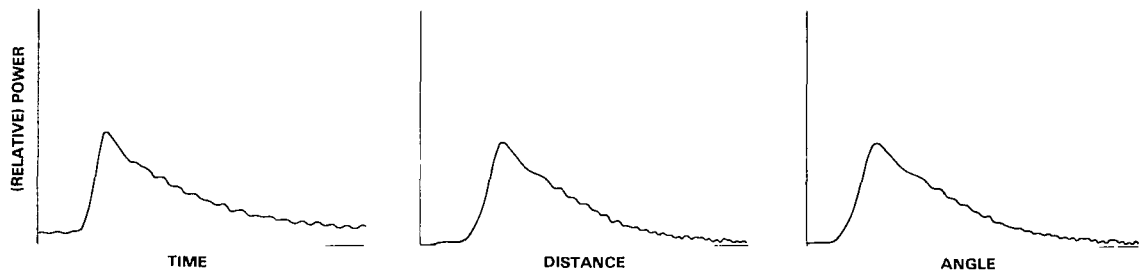


Figure 28. Average power (of 2000 pulses) as a function of time, distance along the surface, and angle from nadir. Data were obtained September 9, 1975, with horizontal polarization and with beam axis 18 degrees from nadir. The aircraft was flying at about 2 km and at 45 degrees with respect to the waves.

CONCLUSIONS

The complete path from an initial sensor concept to the development of a prototype and eventually to the demonstration of its strengths and weaknesses is certainly a long road. JONSWAP-75 represents a major step for the GSFC program because it is a milestone that identifies a field test under well-monitored surface conditions of a prototype short pulse radar. It has been only a little over 2 years from the original idea to the writing of this report. Of course, the radar performance must now be matched against surface "truth." This work is underway and will be reported soon.



REFERENCES

1. Meyers, G. F., "High Resolution Radar Part IV—Sea Clutter Analysis," NRL Report 5191, October 21, 1958.
2. Zamarayev, B. D., and A. L. Kalmaykov, "On the Possibility of Determining the Spatial Structure of an Agitated Ocean Surface by Means of Radars," *Izv. Atmospheric and Ocean Physics*, 5 (1), 1969, pp. 124-127.
3. Tomiyasu, K., "Short Pulse Wide-Band Scatterometer Ocean Surface Signature," Trans. IEEE GE-9 (3) July 1971, pp. 175-177.
4. Brooks, L. W., and R. P. Dooley, "Technical Guidance and Analytical Services in Support of Seasat-A," NASA CR-141399, April 1974.
5. Jackson, F. C., "Directional Spectra of Ocean Waves from Microwave Backscatter," (Proceedings of the URSI Specialist Meeting on Microwave Scattering and Emission from the Earth, Berne, Switzerland, September 1974), pp. 257-272.
6. Le Vine, D. M., et al., "A Short Pulse Radar for Sensing Ocean Wave Structure," (Proceedings of the IEEE/MTS Ocean '75 Symposium, San Diego, September 22 to 25, 1975), pp. 769-774.
7. Eckerman, J., and D. Hammond, "Radar Observation of Ocean Wave Slope Spectra," (IEEE/URSI Symposium, Atlanta, Georgia, June 1974).
8. Yaplee, B. S., A. Shapiro, D. L. Hammond, and E. A. Uliana, "Wave Height Measurements with a Nanosecond Radar," (AGARD Conference Proceedings No. 90, Colorado Springs, Colorado, June 21 to 25, 1971), J. B. Lomax, ed., 1971.
9. Walsh, E. J., "Analysis of Experimental NRL Radar Altimeter Data," *Radio Science*, 9 (8), August 1974, pp. 711-722.
10. Le Vine, D. M., "Monitoring the Sea Surface with a Short Pulse Radar," (Proceedings of the URSI Specialist Meeting on Microwave Scattering and Emission from the Earth, Berne, Switzerland, September 1974), pp. 67-75.
11. Bass, F. G., et al., "Very High Frequency Radiowave Scattering by a Disturbed Sea Surface," Parts I and II, IEEE Trans. AP-16 (5), 1968, pp. 554-568.
12. Barrick, D. E., and W. N. Peck, "A Review of Scattering from Surfaces with Different Roughness Scales," *Radio Science*, 3 (8), 1968, pp. 865-868.

APPENDIX A

FLIGHT LOG

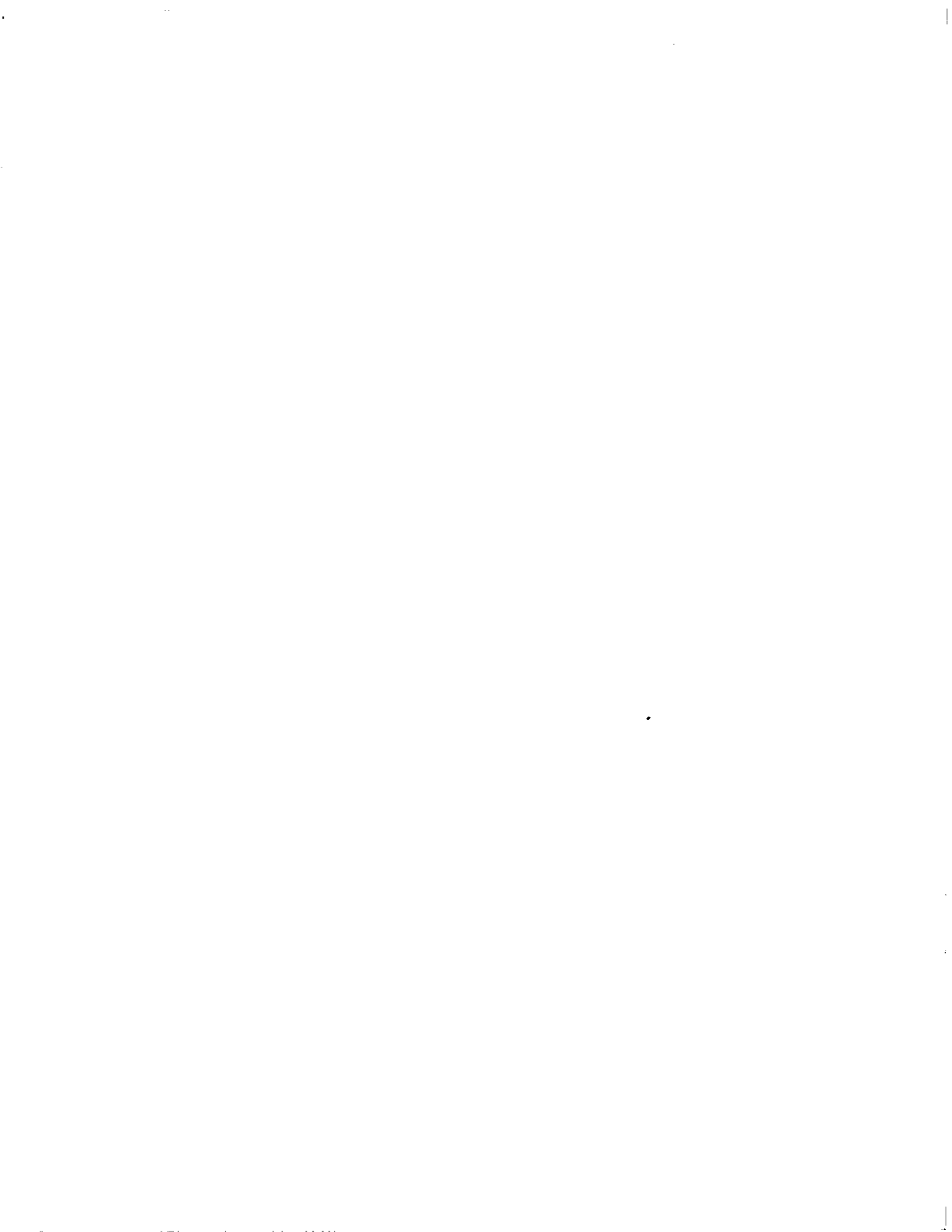


Table A-1
Flight Log

Flight Line/Run	Start (GMT)	Start (Lat.)	Stop (Lat.)	Altitude (km)	Antenna*
Tape/File	Stop (GMT)	Start (Long.)	Stop (Long.)	Ground Speed (m/s)	PAPS†
August 29					
3/3	8:47:55	55° 13.5'	54° 51.7'	3.0	E
1/3	9:02:15	7° 10.5'	8° 6.2'	86	6.49
6/1	9:06:15	54° 51.7'	54° 53.6'	3.0	
1/4	9:19:30	8° 6.2'	6° 49.3'	86	6.49
5/2	9:27:25	54° 41.0'	55° 4.9'	3.0	
2/1	9:39:35	0° 49.0'	7° 31.6'	86	6.49
2/2	9:44:25	55° 1.5'		3.0	
2/2	9:53:51	7° 51.44'		88	6.49
September 2					
2/3	8:24:45	54° 50.4'	55° 27.1'	3.1	H
3/1	8:41:45	6° 41.8'	7° 37.3'	84	6.49
3/1	9:03:24	55° 21.8'	54° 48.8'	3.1	H
3/2	9:06:30	7° 16.8'	8° 19.7'	90	6.49
3/1	9:07:00			3.1	E
3/3	9:08:50			90	6.49
3/2	9:23:30	55° 5.5'	7° 34.7'	3.1	N
3/4	9:28:28	55° 18.2'	7° 10.3'	88	6.49
Radar problem; several shared lines canceled.					
September 4					
3/6	9:56:35	54° 48.6'	54° 39.4'	2.0	E
4/1	10:01:40	7° 55.4'	7° 38.9'	80	6.49
Radar problem; remaining runs canceled.					
September 8					
2/2	13:33:23	55° 0.7'	54° 38.3'	2.0	N
5/1	13:38:34	7° 57.5'	7° 30.7'	80	6.49
5/1	13:51:49	54° 37.7'	55° 6.4'	2.0	N
5/2	13:57:04	7° 48.6'	7° 45.6'	80	6.49

*Antenna beam points at 18° unless otherwise specified.

†PAPS = pulses acquired per second.

Table A-1 (Continued)
Flight Log

Flight Line/Run Tape/File	Start (GMT) Stop (GMT)	Start (Lat.) Start (Long.)	Stop (Lat.) Stop (Long.)	Altitude (km) Ground Speed (m/s)	Antenna* PAPS†
September 8 (Continued)					
2/4	14:38:05	55° 0.2'	7° 59.5'	3.1	N
5/3	14:43:18	54° 21.8'	7° 27.0'	78	6.49
2/5	14:45:34	54° 24.3'	55° 9.4'	3.1	N
5/4	14:50:40	7° 34.0'	8° 16.6'	97	6.49
4/1-2	15:11:20	54° 56.6'		3.0	N
6/1	15:26:15	7° 54.4'		78 (10° bank)	6.49
4/18	16:10:25		55° 12.7'	Same	N
6/2	16:13:30		8° 2.2'		6.49
3/1	16:20:57	55° 7.9'	55° 21.7'	3.0	E
6/3	16:23:00	7° 36.0'	6° 45.6'	82	6.49
3/3	16:52:30	54° 58.6'	55° 3.3'	3.0	E
7/1	16:54:50	8° 0.8'	7° 49.7'	76	6.49
September 9					
3/1	7:25:05	54° 56.8'	55° 6.0'	2.0	E
8/1	7:31:05	7° 42.8'	8° 6.4'	102	6.49
3/2	7:33:20	55° 8.2'	55° 5.2'	2.0	E
8/2	7:35:50	8° 12.9'	8° 4.9'	67	6.49
3/2	7:44:35				
8/3		No data; computer failure			
3/6	9:43:47	54° 56.1'	55° 6.2'	2.0	E
9/1	9:48:30	7° 41.7'	8° 11.6'	104	6.49
5/1	9:53:00	55° 0.1'	55° 5.9'	2.0	E
9/2	9:59:00	8° 10.1'	7° 48.4'	69	6.49
2/4	10:00:00	55° 5.3'	54° 53.6'	2.0	E
9/3	10:05:45	7° 46.6'	8° 4.7'	80	6.49
6/1	10:10:55	54° 55.7'	55° 11.4'	2.0	E
9/4	10:16:55	7° 49.8'	8° 8.3'	100	6.49

*Antenna beam points at 18° unless otherwise specified.

†PAPS = pulses acquired per second.

Table A-1 (Continued)
Flight Log

Flight Line/Run Tape/File	Start (GMT) Stop (GMT)	Start (Lat.) Start (Long.)	Stop (Lat.) Stop (Long.)	Altitude (km) Ground Speed (m/s)	Antenna* PAPS†
September 9 (Continued)					
4/16-19	10:25:35	54° 58.9'	55° 5.5'	2.0	E
10/2-3	10:46:35	7° 53.9'	8° 7.0'	80	6.25
3/7	10:53:00	54° 59.6'	54° 55.0'	2.0	H
11/1	10:58:15	7° 57.8'	7° 41.7'	56	6.25
3/8	10:59:50	54° 54.1'	55° 4.6'	2.0	H
11/2	11:05:10	7° 44.8'	8° 12.5'	100	6.25
5/2	11:10:59	?	?	2.0	H
11/3	11:16:16			73	6.25
2/5	11:17:40	55° 3.3'	55° 15.2'	2.0	H
11/4	11:21:40	7° 51.1'	7° 43.1'	90	6.25
6/2	11:25:20	55° 13.9'	55° 8.0'	2.0	H
11/5	11:27:55	7° 55.7'	7° 55.1'	70	6.25
		Afternoon flights; waves higher.			
6/1	14:38:36	55° 14.2'	55° 3.0'	2.0	E
12/1	14:44:00	8° 3.9'	7° 58.0'	60	6.25
2/6	14:45:35	55° 0.9'	55° 0.1'	2.0	E
12/2	14:51:00	7° 55.9'	7° 36.4'	60	6.25
3/1	14:55:00	55° 5.5'	54° 54.4'	2.0	
12/3	15:00:25	7° 45.0'	7° 58.0'	68	
September 10					
3/1	11:22:25	54° 51.8'	55° 8.0'	3.0	E
13/1	11:24:41	7° 58.1'	7° 49.2'	87	9.09
3/2	11:29:50	55° 7.0'	54° 53.6'	3.0	E
13/2	11:35:24	7° 46.9'	8° 3.5'	86	6.25
5/1	11:37:46	54° 56.6'	55° 3.1'	3.0	E
13/3	11:43:08	8° 7.3'	7° 45.6'	75	6.25
6/1	11:51:40	54° 56.5'	55° 12.7'	3.0	E
13/4	11:56:59	7° 54.6'	8° 6.2'	94	6.25

*Antenna beam points at 18° unless otherwise specified.

†PAPS = pulses acquired per second.

Table A-1 (Continued)
Flight Log

Flight Line/Run	Start (GMT)	Start (Lat.)	Stop (Lat.)	Altitude (km)	Antenna*
Tape/File	Stop (GMT)	Start (Long.)	Stop (Long.)	Ground Speed (m/s)	PAPS†
September 10 (Continued)					
6/2	12:03:15	55° 17.8'	55° 2.1'	3.0	N
14/1	12:08:35	8° 0.8'	7° 55.5'	78	6.25
4/1-4	12:15:45	54° 59.9'	55° 2.5'	3.0 (4.7° bank)	E
14/2 and 15/1	13:00:00	7° 30.7'	7° 36.4'	83-93	6.25
2/5	13:06:32	54° 56.8'	55° 5.6'	3.0	E
16/1	13:11:54	7° 46.8'	8° 15.8'	98	
September 15					
2/5	8:18:43	54° 53.1'	55° 0.0'	2.0	H
17/1	8:21:25	8° 9.0'	7° 47.2'	73	6.25
3/1	8:32:45	54° 52.4'	55° 6.0'	2.0	H
17/2	8:35:25	7° 49.5'	8° 3.9'	80	6.25
3/2	8:36:19	55° 7.4'	54° 55.2'	2.0	H
17/3	8:38:58	8° 2.0'	7° 48.9'	74	6.25
5/1	8:46:17	54° 49.0'	55° 3.0'	2.0	H
17/4	8:51:45	7° 58.9'	7° 55.7'	77	6.25
6/1	08:57:12	54° 57.7'	7° 44.5'	2.0	H
17/6	9:03:25	55° 0.1'	8° 11.5'	80	6.25
4/1-2	9:08:47	55° 2.5'	55° 0.2'	2.0	H
18/1	9:22:58	7° 55.1'	7° 52.7'	74 (7° bank)	6.25
September 16					
3/1	7:40:35	54° 54.1'	55° 3.3'	2.0	N
19/1	7:44:30	7° 34.2'	8° 2.9'	86	12.5
3/2	7:46:15	55° 4.3'	54° 56.4'	2.0	E
19/2	7:51:38	8° 5.7'	7° 44.9'	76	12.5
3/3	7:56:08	54° 55.0'	55° 4.3'	2.0	H
19/3	8:01:30	7° 37.1'	8° 4.7'	88	12.5
2/2	8:14:40	55° 10.9'	7° 39.7'	2.0	N
19/4	8:20:45	54° 57.8'	7° 57.3'	83	12.5

*Antenna beam points at 18° unless otherwise specified.

†PAPS = pulses acquired per second.

Table A-1 (Continued)
Flight Log

Flight Line/Run Tape/File	Start (GMT) Stop (GMT)	Start (Lat.) Start (Long.)	Stop (Lat.) Stop (Long.)	Altitude (km) Ground Speed (m/s)	Antenna* PAPS†
September 16 (Continued)					
2/3	8:26:40	54° 59.1'	55° 12.8'	2.0	E
20/1	8:32:40	7° 55.1'	7° 42.3'	81	12.5
2/4	8:34:25	55° 13.8'	54° 58.0'	2.0	H
20/2	8:41:25	7° 41.0'	7° 58.4'	81	12.5
4/1	8:42:20	54° 57.0'	55° 0.0'	2.0	E
20/3	8:52:15	8° 2.2'	7° 57.3'	88 (4.2° bank)	12.5
4/2	8:56:45	55° 4.5'	55° 9.7'	2.0	E
21/1-2	9:07:55	7° 45.8'	7° 44.5'	74	12.5
No data during afternoon flights.					
September 17					
2/12	14:44:35	54° 53.7'	55° 5.7'	2.0	N
22/1	14:49:17	7° 44.2'	8° 9.7'	96	25
Waves estimated at 8-10 ft.					
3/1	14:58:52	55° 5.7'	54° 53.9'	2.0	N
22/2	15:04:10	7° 45.7'	8° 4.7'	84	25
4/7-9	15:09:56	54° 56.4'	55° 1.8'	2.0	E (31°)
22/3	15:19:05	7° 50.9'	8° 4.2'	82 (15° bank)	25
4/11-12	15:26:20	54° 59.6'	55° 0.9'	2.0	H (31°)
23/1	15:33:00	7° 48.9'	7° 55.1'	74 (15° bank)	25

*Antenna beam points at 18° unless otherwise specified.

†PAPS = pulses acquired per second.

Table A-2
Summary of Estimated Surface Conditions

Date	Windspeed (m/s)	Wave Height (m)
August 29	< 5	< 1
September 2	5	1.0
4	—	—
8	6 to 8	1.0
9 (a.m.)	10	1.5
9 (p.m.)	12	2.0
10	10	1.5
15	9	1.5
16 (a.m.)	7	1.0
16 (p.m.)	10	1.0
17	15	3.0



388 001 C1 U D 770527 S00903DS
DEPT OF THE AIR FORCE
AF WEAPONS LABORATORY
ATTN: TECHNICAL LIBRARY (SUL)
KIRTLAND AFB NM 87117

POSTMASTER: If Undeliverable (Section 158
Postal Manual) Do Not Return

"The aeronautical and space activities of the United States shall be conducted so as to contribute . . . to the expansion of human knowledge of phenomena in the atmosphere and space. The Administration shall provide for the widest practicable and appropriate dissemination of information concerning its activities and the results thereof."

—NATIONAL AERONAUTICS AND SPACE ACT OF 1958

NASA SCIENTIFIC AND TECHNICAL PUBLICATIONS

TECHNICAL REPORTS: Scientific and technical information considered important, complete, and a lasting contribution to existing knowledge.

TECHNICAL NOTES: Information less broad in scope but nevertheless of importance as a contribution to existing knowledge.

TECHNICAL MEMORANDUMS: Information receiving limited distribution because of preliminary data, security classification, or other reasons. Also includes conference proceedings with either limited or unlimited distribution.

CONTRACTOR REPORTS: Scientific and technical information generated under a NASA contract or grant and considered an important contribution to existing knowledge.

TECHNICAL TRANSLATIONS: Information published in a foreign language considered to merit NASA distribution in English.

SPECIAL PUBLICATIONS: Information derived from or of value to NASA activities. Publications include final reports of major projects, monographs, data compilations, handbooks, sourcebooks, and special bibliographies.

TECHNOLOGY UTILIZATION PUBLICATIONS: Information on technology used by NASA that may be of particular interest in commercial and other non-aerospace applications. Publications include Tech Briefs, Technology Utilization Reports and Technology Surveys.

Details on the availability of these publications may be obtained from:

SCIENTIFIC AND TECHNICAL INFORMATION OFFICE

NATIONAL AERONAUTICS AND SPACE ADMINISTRATION

Washington, D.C. 20546